

THIOL-NORBORNENE HYDROGELS WITH TUNABLE MECHANICAL
PROPERTIES FOR ENGINEERED EXTRACELLULAR MATRICES

A Thesis

Submitted to the Faculty

of

Purdue University

by

Han D. Nguyen

In Partial Fulfillment of the

Requirements for the Degree

of

Master of Science in Biomedical Engineering

May 2019

Purdue University

Indianapolis, Indiana

THE PURDUE UNIVERSITY GRADUATE SCHOOL
STATEMENT OF THESIS APPROVAL

Dr. Chien-Chi Lin, Chair

Department of Biomedical Engineering

Dr. Hiroki Yokota

Department of Biomedical Engineering

Dr. Dong Xie

Department of Biomedical Engineering

Approved by:

Dr. Julie Ji

Head of the School Graduate Program

ACKNOWLEDGMENTS

I would like to thank my thesis advisor, Dr. Chien-Chi Lin, without whom this thesis would not be possible. Dr. Lin has taught me valuable research experiences as well as critical thinking skills which I will always be grateful for.

I would also like to thank my thesis committee members, Dr. Hiroki Yokota and Dr. Dong Xie for their time and helpful feedbacks.

In addition, I would like to thank my colleagues: Hung-Yi Liu, Matt Arkenberg, Kevin Peuler, Dustin Moore, and Hunter Johnson for the helpful research discussions.

Thanks also go to Mrs. Sherry Clemens for her assistance with the formatting of this thesis. Lastly, thanks to all my friends and family for their encouragement and support throughout my Masters.

TABLE OF CONTENTS

	Page
LIST OF TABLES	vii
LIST OF FIGURES	viii
LIST OF ABBREVIATIONS	xi
LIST OF NOMENCLATURE	xiii
ABSTRACT	xiv
1 INTRODUCTION	1
1.1 Mechanical Properties of Extracellular Matrix (ECM)	1
1.1.1 Cells Behaviors in Response to Changes in ECM Elasticity	1
1.1.2 Cell Behaviors in Viscoelastic ECM	3
1.1.3 Engineered Biomimetic Materials to Recapitulate ECM	4
1.2 In situ Formation of Thiol-norbornene Hydrogel via Horseradish Peroxidase	5
1.2.1 Thiol-norbornene Photopolymerization	5
1.2.2 Horseradish Peroxidase-Catalyzed in situ Hydrogels	6
1.3 Enzyme-induced Dynamic Stiffening of Hydrogels	9
1.4 Hydrogels with Tunable Viscoelasticity	9
1.4.1 Boronic acid-containing Hydrogels	9
1.4.2 Mushroom Tyrosinase-triggered Boronate Ester Formation in the Presence of Ascorbic Acid	11
2 OBJECTIVES	13
2.1 Objective 1: HRP-mediated Crosslinking of Thiol-norbornene Hydrogels	13
2.2 Objective 2: Mushroom Tyrosinase-triggered Boronic acid-DOPA Dynamic Covalent Bonds Formation	14
3 MATERIALS AND METHODS	16

	Page
3.1 General Materials	16
3.2 Macromers Synthesis	16
3.3 Peptide Synthesis and Purification	17
3.4 HRP-mediated Thiol-norbornene Hydrogel Fabrication	17
3.5 Rheometry	18
3.6 Norbornene and Thiol Consumption	19
3.7 Characterization of Gel Fraction	19
3.8 In-gel Oxygen Measurements	20
3.9 3T3 Fibroblasts Encapsulation	20
3.10 Dynamic Stiffening of Enzymatically Crosslinked PEG-peptide Hydrogels	21
3.11 Functionalization of Gelatin with Boronic Acid and Hydroxylphenolic Acid	21
3.12 Mushroom Tyrosinase-triggered Boronic acid DOPA Dynamic Covalent Bonds Formation	22
3.13 MBTH colorimetric assay to detect dopachrome formation	22
3.14 BA-conjugated Lucifer Yellow Fluorescent Assay to Detect DOPA- formation	22
4 RESULTS AND DISCUSSION	24
4.1 HRP-mediated Thiol-norbornene Hydrogels	24
4.1.1 Characterization of HRP-mediated Thiol-norbornene gelation	24
4.1.2 Tyrosine-assisted enzymatic crosslinking of PEG-peptide hy- drogels	28
4.1.3 HRP/GOX Dual Enzymatic Thiol-norbornene Gelation	30
4.1.4 Enzymatically Crosslinking of Gelatin-based Thiol-norbornene Hydrogels	33
4.1.5 Dynamic Stiffening of Enzymatically Crosslinked PEG-peptide Hydrogels	34
4.1.6 Cell Encapsulation and Dynamic Stiffening of Cell-laden Hydrogels	35
4.2 MT-mediated Viscoelastic Hydrogel Boronic Acid	38

	Page
4.2.1 Controlled Formation of L-DOPA Product using MT and Ascorbic acid	39
4.2.2 Characterization of Primary Elastic Network	41
4.2.3 Tunable Viscoelastic Hydrogels via MT and AA	41
5 SUMMARY AND RECOMMENDATIONS	44
5.1 Summary	44
5.2 Recommendations	45
LIST OF REFERENCES	46
APPENDIX	54

LIST OF TABLES

Table	Page
1.1 HRP-mediated Hydrogels Applications	7

LIST OF FIGURES

Figure	Page
1.1 Catalytic cycle of Horseradish Peroxidase in the presence of H_2O_2	8
1.2 Boronic interaction with 1,2 - diol to form dynamic covalent boronate ester bond.	10
1.3 Schematic of MT-mediated oxidation in the presence of AA.	12
2.1 Schematic of HRP-mediated thiol-norbornene polymerization.	14
2.2 Schematic of mushroom tyrosinase-induced viscoelastic hydrogel.	15
4.1 Tilt test of HRP-mediated thiol-norbornene hydrogel. All components: 200 U/mL HRP, 0.5 mM H_2O_2 , 3.5 wt% PEG8NB, and 14 mM DTT.	24
4.2 In situ rheometry of HRP-initiated thiol-norbornene gelation (3.5 wt% PEG8NB, 14 mM DTT, 200 U/ml HRP, 0.5 mM H_2O_2).	25
4.3 (A) Thiol conversion profiles as a function of reaction time. (B) Norbornene conversion as a function of thiol-norbornene ratio.	26
4.4 Effect of (A) HRP concentrations and (B) H_2O_2 concentration on shear moduli of PEG8NB-DTT hydrogels. Gelation was formed with 3.5 wt% PEG8NB, and 14 mM DTT, $R_{thiol/ene}=1$. $N = 3$, mean \pm SEM). (C) Strain-sweep rheometry of thiol-norbornene hydrogels formed with different macromer contents (3, 3.5, and 4 wt%. $R_{thiol/ene} = 1$). ($n \geq 3$, Mean \pm SEM, *** $p < 0.001$).	27
4.5 HRP-crosslinked thiol-norbornene hydrogel with a diameter of 4 mm and a length of 15 mm (200 U/mL HRP, 0.5 mM H_2O_2 , 3.5 wt% PEG8NB, and 14 mM DTT).	28
4.6 Proposed schematic of thiol radical generation via tyrosine residues.	29
4.7 Effect of (B) tyrosine concentration and (C) thiol to norbornene ratios on the shear moduli of hydrogels. Hydrogels were crosslinked at 1 U/ml HRP, 0.5 mM H_2O_2 ($n=3$, Mean \pm SEM, *** $p < 0.001$).	30

Figure	Page
4.8 (A) Effect of glucose concentrations on shear moduli of dual enzyme-crosslinked thiol-norbornene hydrogels (1 U/mL HRP, 10 U/ml GOX, 3 wt% PEG8NB, and 12 mM CYGGGYC, $R_{thiol/ene} = 1$). (B) Oxygen contents within hydrogels formed by HRP/GOX/glucose (1 U/ml HRP, 1 U/mL GOX, 10 mM glucose) and HRP/ H ₂ O ₂ (1 U/mL HRP, 0.5 mM H ₂ O ₂).	31
4.9 (A) Gel fraction (B) Mass swelling ratio and Storage Moduli G' of hydrogels formed with HRP/H ₂ O ₂ , HRP/GOX and UV light-mediated thiol-ene photopolymerization. (3.5 wt% PEG8NB-DTT, $R_{thiol/norbornene} = 1$, n = 3, mean ± SEM, * p<0.05). HRP/H ₂ O ₂ gels were formed with 200 U/ml HRP and 1 mM H ₂ O ₂ ; HRP/GOX gels were formed with 200 U/ml HRP, 10 U/ml GOX, and 10 mM glucose. UV light-mediated gels were formed with 1 mM LAP, and UV light at 365 nm wavelength for 2 minutes. . . .	33
4.10 Effect of gelatin content (A) and thiol to norbornene ratio (B) on the moduli of GelNB-PEG4SH hydrogels (100 U/ml HRP, 10 U/ml GOX, 10 mM glucose) (n≥3, Mean ± SEM, *p<0.05, ***p<0.001).	34
4.11 (A) Schematic of MT-induced post-gelation dynamic crosslinking. (B) Photographs of enzymatically crosslinked PEG-peptide (2.5 wt% PEG8NB and KCYGGYGGYCK (3Y) thiol-norbornene hydrogels pre- and post-stiffening. Gel crosslinking was initiated by 1 U/mL HRP, 10 U/mL GOX, and 10mM glucose. Stiffening was induced by incubating the swollen gels in PBS containing 1 kU/mL MT. (C) Shear moduli of hydrogels pre- and post-stiffening. HRP = 1 U/ml, HRP/H ₂ O ₂ hydrogels were made with 3 wt% PEG8NB, while HRP/GOX-glucose were made with 2.5 wt% PEG8NB to give modulus around 1000 Pa. (n=3, Mean ± SEM, ***p<0.001).	35
4.12 (A) Live/Dead staining images of 3T3 cultured in GelNB-PEG4SH hydrogels 24 hrs after encapsulation. Hydrogels were formed with 1.5 wt% GelNB-PEG4SH, 100 U/ml HRP, and 0.5 mM H ₂ O ₂ , modulus G' = 1000 Pa. (B) Fluorescence staining images of spread 3T3 at day 1 and day 8. .	36
4.13 Live/Dead and Fluorescence images of 3T3 at Day 2 (24 hours after stiffening) and Day 8. Stiffened group were treated with 1 kU/ml tyrosinase for 6 hours on day 1. Hydrogels were made with 3 wt% PEG8NB-KCYGGYGGYCK, 1 U/ml HRP, 0.5 mM H ₂ O ₂ , G' ~1500 Pa.	38
4.14 MBTH assay to detect dopachrome formation in the presence of MT and AA. Solution containing 10 mM tyrosine, 0.2 U/ml MT, 2 mM MBTH and various concentration of AA was used.	39

Figure	Page
4.15 (A) Selective recognition of DOPA by Luc-BA fluorescent molecule. (B-C) Normalized emission intensity of Luc-BA at different concentration of (B) Dopamine and (C) GelNB-HPA in the presence of MT, AA. Excitation wavelength is 430 nm.	40
4.16 3 wt% GelNB-BA/3 wt% GelNB-HPA/PEG4SH hydrogels formed via LAP and UV-light (365 nm, 2 minutes) at different thiol-norbornene ratios.	41
4.17 Effect of AA on MT-mediated stiffening. Hydrogels were made from 3 wt% GelNBHPA/3 wt% GelNB-BA/PEG4SH ($R_{thiol/nor} = 0.75$). Hydrogels were incubated in 1 kU/ml MT for 6 hours in the presence and absence of 5 mM AA.	42
4.18 (A) Storage moduli and loss moduli (B) $\tan(\delta)$ of 3 wt% GelNB-BA/ 3wt% GelNB-HPA/PEG4SH hydrogels ($R_{thiol/norbornene} = 0.75$) treated with no MT; 1 kU/ml MT; and both 1 kU/ml MT, 5 mM AA.	43
A.1 ^1H NMR spectra showing the consumption of the alkene proton (5.9-6.25 ppm) on the norbornene functional groups at different $R_{thiol/norbornene}$	54

LIST OF ABBREVIATIONS

AA	Ascorbic acid
BA	Boronic acid
ddH ₂ O	Double distilled water
DMEM	Dulbeccoss Modified Eagles medium
DOPA	Dihydroxyphenylalanine
DTT	Dithiothreitol
EDC	1-Ethyl-3-(3-dimethylaminopropyl)-carbodiimide
FAK	Focal Adhesion Kinase
FBS	Fetal Bovine Serum
Gel	Gelatin
GOX	Glucose oxidase
H ₂ O ₂	Hydrogen Peroxide
HA	Hyaluronic acid
hMSCs	Human mesenchymal stem cells
HPA	4-hydroxyphenyl acetate
HRP	Horseradish Peroxidase
HUVEC	Human umbilical vein endothelial cell
LAP	Lithium aryl phosphonate
LOX	Lysyl oxidase
Luc	Lucifer Yellow
MBTH	3-Methyl-2-benzothiazolinone hydrazine
MT	Mushroom Tyrosinase
NB	Norbornene
NHS	N-hydroxysuccinimide

PAIN	Pancreatic Intraepithelial Neoplasia
PDAC	Pancreatic Ductal Adenocarcinoma
PEG	poly(ethylene glycol)
PEG8NB	8-arm poly(ethylene glycol)-norbornene
TFA	Trifluoroacetic acid
TIS	Trisisopropylsilane
Tyr	Tyramine
UV	Ultraviolet
YAP	Yes-associated protein 1

LIST OF NOMENCLATURE

G'	Storage Modulus
G''	Loss Modulus
$\text{Tan}(\delta)$	Loss tangent
$W_{dry,1}$	First dry weight
$W_{dry,2}$	Second dry weight
$W_{swollen}$	Swollen mass
Q	Mass swelling ratio

ABSTRACT

Nguyen, Han D. M.S.B.M.E., Purdue University, May 2019. Thiol-Norbornene Hydrogels with Tunable Mechanical Properties for Engineered Extracellular Matrices. Major Professor: Chien-Chi Lin.

The extracellular matrix (ECM) governs many cellular processes through biochemical and mechanical cues. Particularly, the effect ECM mechanical properties on cells fate has been well established over the years. Many hydrogel systems have been used to mimic the dynamic stiffening processes occurring in ECM. However, changes in ECM stiffness does not fully recapitulate the mechanics of native ECM, as viscoelasticity is also a major factor contributing to ECM dynamic property. This thesis describes the design and characterization of an enzyme-crosslinked hydrogel system that is not only capable of being stiffened on demand, but also can be tuned to obtain viscoelasticity. The first objective of this thesis was to utilize horseradish peroxidase (HRP) to crosslink thiol-norbornene hydrogel and use mushroom tyrosinase (MT) to create secondary DOPA-dimer crosslinks that stiffened the hydrogel. The cytocompatibility of HRP-mediated thiol-norbornene gelation and the effect of stiffening on cell fate was evaluated. The second objective of this thesis represented the first step towards developing a hydrogel system whose viscoelasticity could be dynamically tuned. Thiol-norbornene hydrogel was designed to yield dynamically adaptable boronic ester bonds via partial enzymatic reaction. Thiol-norborne hydrogel was made to contain hydroxyl phenol as well as boronic acid residues within its network. MT, in this case was used to oxidize the hydroxy phenol moieties into DOPA, which then complexed with boronic acid, created dynamic bonds, introducing viscoelasticity to an initial elastic hydrogel.

CHAPTER 1. INTRODUCTION

1.1 Mechanical Properties of Extracellular Matrix (ECM)

The interactions between cells and their ECM have been extensively studied because the ECM not only provides structural support for cells but also transduces mechanical and biochemical signals to regulate cellular activities [1]. Recent advances in biomaterials science and engineering have permitted scientists to elucidate important ECM components as well as the mechanisms by which ECM influences normal cellular processes such as migration, differentiation, as well as pathological events like cancer [2, 3], fibrosis [4], and wound healing [5]. There has been growing evidences indicating that changes in the ECM mechanical properties greatly affect cells organization and functions. Particularly, excessive collagen I deposition/crosslinking orchestrated by activated fibroblasts during fibrosis and in tumor progression is believed to contribute significantly to the aberrant mechanosensing and abnormal cell behaviors [6].

1.1.1 Cells Behaviors in Response to Changes in ECM Elasticity

ECM remodeling during cancer progression has been observed in many tumor types and used as a hallmark in cancer progression [2, 3, 6]. Tumor tissues have abnormally high stiffness, which is known to fosters cancer cell metastasis and drug resistance [3]. Depending on the cancer types, the stiffness of tumor environment can be 2-fold up to 10-fold higher than noncancerous tissue [2, 7]. In one report, the Weaver group showed that the breast tumor subtypes, Basal-like and HER2 had

stromal invasion fronts that were up to 4-fold stiffer in elastic modulus when comparing to the normal adjacent tissues and the non-invasive regions at the core [2]. It is believed that the higher matrix stiffness was a result of progressive deposition and remodeling of type I collagen within the ECM [2]. Immunohistochemistry analysis also revealed, among other breast cancer subtypes including luminal A and B, Basal-like and HER2 had the highest levels of activated integrin β -1, focal adhesion kinase (FAK), as well as the highest nuclear level of Yes-Associated Protein (YAP). Collectively, these experimental observations suggested that aggressive cancer cells were more mechanically-activated than non-invasive and benign ones [2]. Similarly, Rice et al. found that the progression of pancreatic ductal adenocarcinoma (PDAC) from normal pancreas tissues correlates strongly with the increase in tissue fibrotic rigidities. The Young's modulus of healthy pancreas was below 1000 Pa, while pancreatic intrapitheilia neoplasia (PanIN), precursor of PDAC had a stiffness around 2000 Pa, and PDAC's stiffness was around 4000 Pa. It was also discovered that higher matrix stiffness induced tumor chemoresistance and promoted epithelial-mesenchymal transition (EMT) of pancreatic cancer cells [3]. Changes in ECM mechanics also plays a key role in mesenchymal stem cells (MSCs) differentiation [8]. Wang et al. conducted a study where hMSCs were encapsulated within gelatin-based hydrogels with different stiffness [9]. The results showed that, even without adding any biochemical cues, cells encapsulated within soft hydrogels (300 Pa) exhibited higher neuronal commitment than in stiffer hydrogels (800 Pa). Specifically, the levels of neuronal protein markers, including neurofilament light chain (NFL), neurofilament heavy chain (NFH), microtubule associated protein 2 (MAP2), and neuron-specific marker β 3 tubulin were all upregulated [9]. Moreover, significant difference in focal adhesion and F-actin rearrangement between the soft and stiff groups were also observed. Cells were more scattered in soft gels and more organized in stiff ones. These results suggested that hMSCs can indeed sense the stiffness of the surrounding environment and respond to subtle difference in gel moduli (i.e., 300 pa vs 800 Pa) [9]. ECM elasticity also regulates stem cells renewal. As reported by Gilbert et al., muscle

stem cells (MuSCs) cultured in substrate with 12 kPa modulus experienced higher survival rate and delayed differentiation [10]. On the contrary, MuSCs grown within a much stiffer substrate (>42 kPa) over time lost their stemness and regenerative potential [10].

1.1.2 Cell Behaviors in Viscoelastic ECM

In addition to matrix elasticity, ECM viscoelasticity can also impact cellular response. Many human tissues like adipose, liver, and brain are viscoelastic and can stress-relax more than 50% within 10s [11]. This means that when cells exert forces onto their matrices, the mechanical energy is not stored, like in many elastic materials. Instead, the force is dissipated over time throughout the network via ECM reorganization, which allows cells to migrate and spread [12]. Viscoelastic materials have been reported to better maintain cell viability and to promote cell-matrix interaction, spreading, and migration [13]. In one example, Chaudhuri et al. encapsulated 3T3 fibroblasts in non-degradable, nanoporous RGD-couple alginate hydrogels with varying stress-relaxation rate to show that at the same initial elastic modulus, fast relaxing gels enhanced cell spreading and proliferation [13]. When the same experiment was performed using MSCs, osteogenesis was also significantly improved with increased stress-relaxation rate [11]. The effect of stress relaxation on osteogenic differentiation was hypothesized to be mediated through ECM ligands, where cycles of strain and stress exerted on network by cells led to matrix reorganization, cell shape change, and clustering of RGD [11]. In another research, the Mooney group has established that stress relaxation rate regulated myoblast spreading and proliferation [14]. The same group has also reported a new mode of protease-independent cell migration when cells were surrounded by stress relaxing viscoelastic hydrogel network [15]. Human breast adenocarcinoma MDA-MB-231 cells encapsulated in a nanoporous alginate-basal membrane interpenetrating network hydrogel were shown to extend invadopodia protrusion to physically widening the mesh size of surrounding

gel network to enable migration. Longer protrusions were observed in gels with higher plasticity, suggesting matrices that can easily be deformed promote more spreading and invasion [15]. Overall, these results show that, in addition to changes in ECM stiffness, viscoelasticity is another parameter to take into consideration while design biomimetics materials.

1.1.3 Engineered Biomimetic Materials to Recapitulate ECM

Over the past years, efforts have been dedicated to develop hydrogel systems that can be stiffened on demand to prompt specific cell response. For instance, instead of static soft or stiff hydrogel network, hydrogels capable of being stiffened over time were employed to tailor hMSCs fate [4]. User controlled hydrogel stiffening are typically achieved by employing a secondary crosslinking. As presented by Guvendiren and Burdick, methacrylated hyaluronic acid-dithiolthreitol (DTT) hydrogel can be formed via Michael type addition with off stoichiometric thiol to ene ratio [4]. The extra methacrylate moieties can then further undergo crosslinking via radical polymerization to increase stiffness of a hydrogel (G' was increased from 3 to 30 kPa). hMSCs encapsulated within hydrogel experienced different degrees of stiffening exhibited different lineage commitment. Specifically, hMSCs cultured within 10-fold stiffened hydrogels increased cell spreading and possessed much stronger actin fibres. Although cultured in bipotential media supporting both adipogenesis and osteogenesis, the cells showed osteogenesis markers immediately after stiffening. Notably, stiffening at day 7 resulted in no differentiation if hMSCS had already differentiated toward adipogenic lineage, however, if cells had not differentiated, they would go through osteogenesis as a result of stiffening [4]. More recently, Liu et al. has developed a dynamic cell-laden hydrogel that can be stiffened via flavin mononucleotide and visible light to observe tumorigenesis [16]. In short, PEG8NB hydrogel was crosslinked with peptides containing tyrosine residues. FMN and visible light were employed to initiate secondary di-tyrosine crosslinking, which subsequently stiffened

the hydrogel. Cancer associated fibroblasts cultured on stiffened region were said to be significantly more activated with increased spreading morphology and nuclear translocation of YAP. The impacts of ECM mechanics on cellular activities have been well established [16]. Gaining knowledge from the projects mentioned above, the overarching goal of this thesis was to develop a versatile hydrogel system that not only captures key changes in ECM remodeling (e.g., stiffening), but also displays time-dependent response to mechanical loading and deformation (e.g., stress-relaxation).

1.2 In situ Formation of Thiol-norbornene Hydrogel via Horseradish Peroxidase

1.2.1 Thiol-norbornene Photopolymerization

Hydrogel can be crosslinked via a myriad of reactions, including Michael type addition [4, 17, 18], Schiff-based [19, 20], DielsAlder [21], and alkyne-azide cyclo-addition [22]. Owing to its tunability, orthogonality, and biocompatibility, one chemistry that is highly popular amongst biomaterial scientists is the thiolnorbornene click reaction. The UV-mediated thiol-norbornene reaction was developed by the Anseth group to fabricate hydrogels that can be used as biomimetic material [23]. Upon UV irradiation with an initiator, a hydrogen on the thiol molecule is abstracted, yielding a thiyl radical. The thiyl radical can then propagate to the C=C on the norbornene groups, creating a carbon-center radical [23]. This intermediate transfers its radical onto another thiol molecule to give the final thioether bond and another thiyl radical to continue the thiol-norbornene reaction until depleting the functional groups [23]. The thiol-norbornene reaction possesses several attractive features, such as fast process, no oxygen inhibition, and most importantly, orthogonality in macromer crosslinking. Light-mediated thiol-norbornene reaction also offers precise spatial-temporal controls in gelation kinetics, allowing users to easily tune hydrogel properties both before and after gel formation [24]. Up to this point, all thiol-norbornene hydrogels are strictly fabricated via photo-polymerization with either UV or visible light [23, 25]. The use

of light-mediated reaction, however, has its limitations, especially in many in vivo experiments where light penetration is restricted only near the surface of the tissue [26]. It would be advantageous if these limitations can be overcome by employing an enzymatic reaction that can crosslink hydrogel rapidly under physiological condition without dimension limitation.

1.2.2 Horseradish Peroxidase-Catalyzed in situ Hydrogels

Horseradish peroxidase (HRP) has emerged as a powerful enzyme for in situ crosslinking of hydroxyl-phenol-modified (e.g., hydroxyphenylacetic acid (HPA), tyramine, or tyrosine) polymers, including silk [27,28], hyaluronic acid [29], gelatin [30], poly (vinyl alcohol) [31], and poly (ethylene glycol) (PEG) [32,33]. Table 1.1 summarizes notable HRP-crosslinked hydrogels with applications ranging from drug delivery [24,34,35] and tissue engineering [36–40] to wound dressing [30,31].

HRP initiates hydrogel crosslinking by generating radical species in the presence of hydrogen peroxide (H_2O_2), which can be provided with either exogenous H_2O_2 or by supplying indirectly through a secondary reaction. When comes in contact with H_2O_2 , a strong oxidizing agent, HRP loses two electrons and becomes activated Compound 1, which is two oxidizing equivalents above the resting state. In the first one-electron reduction step, Compound 1 reacts with a reducing substrate AH, to produce Compound 2, a species that is one oxidizing equivalent above resting state. Finally, in the second one-electron reduction step, Compound 2 gains one more electron from the reducing substrate to return back to the inactivated HRP [41]. As HRP is being continuously regenerated, the reaction stops only when H_2O_2 is no longer available.

Table 1.1: HRP-mediated Hydrogels Applications

Materials	Cell type	Application	Note	Reference
Gelatin-HPA	Human Dermal Fibroblast	Cell encapsulation	No exogenous H ₂ O ₂ used	[36]
Gelatin-Tyr, HA-Tyr, Alginate-Tyr	HeLa and 10T1/2	3-D Bioprinting	Low [H ₂ O ₂], > 95% cell viability	[37]
Alginate-Tyr	10T1/2	Cell encapsulation	No H ₂ O ₂ used, No GOX/glucose	[38]
Gelatin-based	Dendritic cells	Sustained release of oncolytic adenovirus and dendritic cells for cancer immunotherapy		[34]
Silk-collagen based	Fibroblasts encapsulation	3D matrix to support human skin equivalent with nervous system components		[39]
Gelatin-oxidized beta-cyclodextrin-Tyr	No cell	Injectable hydrogel for improved hydrophobic drug delivery (dexamethasone and curcumin)		[35]
Gel-HPA	No cell	Releasing H ₂ O ₂ to kill drug resistant bacteria on wounds	GOX/glucose used to gradually release H ₂ O ₂	[30]
Gel-HPA	HUVEC	Releasing H ₂ O ₂ to enhance endothelial cell activities and neovascularization		[40]
PVA-Tyr	No cell	Sprayable wound dressing utilizing glucose available in wound exudate	No exogenous H ₂ O ₂ used	[31]
Thiolated-linear polyglycidol	No cell	Delivery proteins using nanogels	Gels formed through disulfide bonds at basic pH	[24]

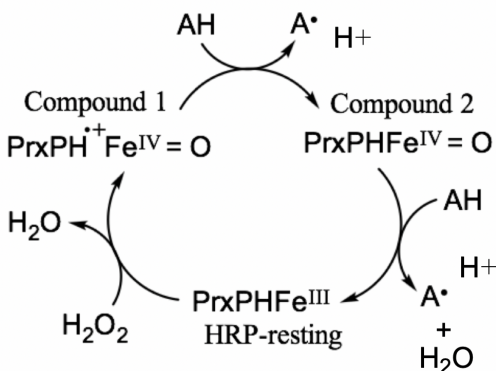


Fig. 1.1: Catalytic cycle of Horseradish Peroxidase in the presence of H_2O_2 .

In addition to direct supply, H_2O_2 can be generated by Glucose oxidase (GOX) with glucose as its substrate. Kim et al. have reported a gelatin based hydrogel system initiated by dual enzymes HRP-GOX with controlled mechanical property and gelation time via tuning concentrations of GOX and glucose [36]. The study has also demonstrated that hydrogels made with the HRP-GOX enzyme pair were cytocompatible for encapsulating human dermal fibroblasts. More recently, Gantumur and colleagues have reported a method to form hydrogel using HRP as both the catalyst and supplier of H_2O_2 [38]. The research group hypothesized that HRP can oxidize the thiol moieties on itself to generate H_2O_2 . This self-oxidization can be accelerated with high concentration of glucose and HRP [38]. HRP can also catalyze Reversible Addition-Fragmentation chain Transfer (RAFT) polymerization [42], as well as thiol-allylether [26], and tetrazine-norbornene [43] hydrogel crosslinking. As demonstrated by Zavada et al., PEG diallyl ether (PEGDAE) and ethoxylated trimethylolpropane tri(3-mercaptopropionate) (ETTMP) can be successfully crosslinked to form hydrogels with HRP and H_2O_2 through thiol-ene reaction. However, the gelation of HRP-initiated thiol-allylether gelation required high HRP concentrations (~ 100 - 300 U/mL) and H_2O_2 (~ 100 mM). Employing HRP to initiate thiol-norbornene reaction provides alternative routes to create thiol-norbornene hydrogels, eliminating photopolymerization limitations, making the reaction more translatable in many in vivo applications.

1.3 Enzyme-induced Dynamic Stiffening of Hydrogels

It has been well-established that excessive collagen deposition and crosslinking are the reasons behind ECM stiffening in diseased tissues. As reported by Levental et al., inhibition of lysyl oxidase (LOX)-mediated collagen crosslinking significantly decreased fibrosis and delayed tumor progression [44]. Enzymatic reactions have been exploited as a means to stiffen cell-laden hydrogels. This approach for hydrogel stiffening may be more relevant than light-mediated stiffening because enzymatic reactions mimic the mechanism and timescale of enzyme-mediated tissue stiffening. Mushroom tyrosinase is a polyphenol oxidase that is widely used to crosslink hydroxyl phenol in to hydrogel as well as to stiffen hydrogel. In the presence of oxygen, MT can oxidize hydroxyl phenol moieties into L-DOPA, then to dopaquinone, dopachrome, and eventually DOPA-dimers [45]. Choi et al. used MT to modify tyrosine residues on gelatin to DOPA, which can coordinate with Fe^{3+} to form hydrogel for wound healing application. DOPA residues were reported to bind to tissue surface through formation of H-bond and electrostatic interaction, thus enhancing hydrogel dressing adhesiveness [45]. Apart from forming hydrogel, Liu et al. demonstrated tyrosinase can be used to stiffen hydrogel and investigate PDAC response to matrix modification. It was discovered matrix stiffening coupled with the incorporation of hyaluronic acid significantly increased the migratory phenotype of PDAC cells types, making the cells more invasive. MT provided a perfect tool for temporal controlling of matrix stiffening; due to its slow diffusion time into hydrogels, the timescale of ECM modification experienced by cells can be more closely mimicked.

1.4 Hydrogels with Tunable Viscoelasticity

1.4.1 Boronic acid-containing Hydrogels

Boronic acid (BA) can form dynamic covalent bond with molecules contain diol moieties, such as dopamine, catechol, or sugar molecules such as glucose, mannose,

ascorbic acid, etc. (Fig 1.2) [46]. Boronic acid-diol complex is highly desired in the biomedical field due to rapid association and dissociation dynamics, nontoxicity, and its mechanical resilience comparing to the physical crosslinked counterparts. The equilibrium or binding affinity between boronic acid and diol functional groups depends greatly on the pH of the reaction buffer and the pKa of the boronic acid [22,47]. The complex is favored only when pH value is above the pKa. Reducing pH to lower than pKa or adding stronger affinity binder for diol can cause dissociation of boronate ester bond. Boronic acid-diol interaction has also been explored to create self-healing materials. When the boronate bonds are broken by mechanical forces, the reversible boronic acid/diol binding can rearrange to form new bond that heals the damage [47, 48].

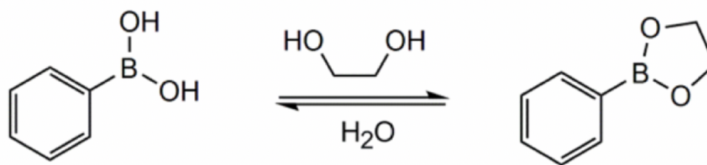


Fig. 1.2: Boronic interaction with 1,2 - diol to form dynamic covalent boronate ester bond.

Incorporating boronate ester bond into hydrogels introduced many advantageous functions to the network. Boronic acid-containing hydrogel has been employed in many applications, ranging from biosensor [46], drug delivery [49] to self-healing materials for dynamic cell culture [22,47]. For example, Yesilyurt et al. prepared glucose responsive PEG-based hydrogels using phenylboronic acid and cis-diol derivatives [50]. The hydrogels were capable of releasing Immunoglobulin G (IgG) and insulin upon exposure to high glucose concentration. Utilizing the shear thinning properties of the boronic-diol bonds, the hydrogel can also be injected subcutaneously for therapeutics delivery [50]. More recently, Smithyer et al. demonstrated that boronic-diol complex can be utilized to generate self-healing gels to probe directional

cell migration and invasion [47]. Two cell-laden boronic ester hydrogels separately encapsulating fibroblasts and breast cancer cells were fused together to generate a co-culturing hydrogel block. The interaction between the two cells types was monitored, especially at the healed interfaced [47]. The results showed that while both cell types were able to cross the healed interface and migrate toward one another, breast cancer cells migrated in a longer distance than fibroblast cells. As mentioned previously, the binding affinity of the boronic acid to diol depends greatly on pKa of the boronic acid group. Exploiting this knowledge, Accardo and Kalow reported a hydrogel system possessing boronic ester bonds that can be reversed using visible light, where light exposure would alter pKa of boronic acid moieties, hence, influences the equilibrium of the complex [51]. To achieve this, BA was conjugated with azobenzene groups, under light exposure, the azo moieties can switch between E and Z isomers, resulting in changes in pKa of BA [51]. Furthermore, the reversible bond can be used to mimic the dynamic mechanical properties found in native tissue. The Anseth group reported a fast stress-relax hydrogel construct containing both permanent non-degradable azide-alkyne bonds and dynamic covalent boronic ester bonds that can promote hMSCs spreading through physical remodeling of the surrounding network [22]. Furthermore, by varying the phenylboronic acid derivatives with different pKa, stress relaxation rate of materials can be systematically tuned over a broad range of timescales to be physiologically relevant to various cellular development states and cell types [52].

1.4.2 Mushroom Tyrosinase-triggered Boronate Ester Formation in the Presence of Ascorbic Acid

Recently, Montanari et al. introduced a technique to conjugate boronic acid to tyrosine through enzymatically converting tyrosine into catechol [53]. During the treatment of tyrosine with mushroom tyrosinase, ascorbic acid (or vitamin C) was added as a reducing agent to stop tyrosine oxidation at the catechol stage without

being oxidized further to dopaquinones and dopachrome (Figure 1.3) [53]. The newly formed DOPA could immediately complex with boronic acid to create a reversible bond. This conjugation technique was reported to be advantageous for sustained release of tyrosine-containing protein and drugs. Using this knowledge, we hypothesized that a purely elastic hydrogel containing tyrosine and boronic acid moieties can be converted in to a gel with tunable viscoelasticity by forming a secondary boronic ester network.

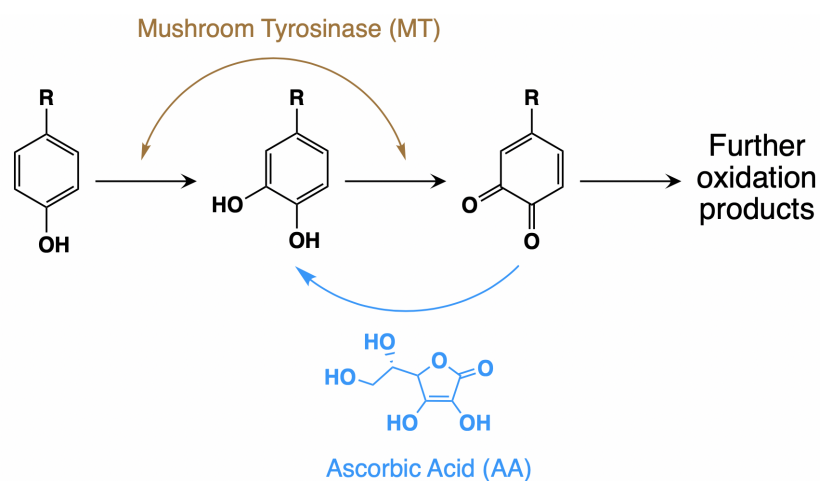


Fig. 1.3: Schematic of MT-mediated oxidation in the presence of AA.

CHAPTER 2. OBJECTIVES

2.1 Objective 1: HRP-mediated Crosslinking of Thiol-norbornene Hydrogels

The first objective of this thesis was to develop an innovative way to enzymatically crosslink thiol-norbornene hydrogel. The thiyl radicals required for thiol-norbornene gelation can be generated by HRP and H_2O_2 . The system will eliminate the limitations of photopolymerization while maintaining the reaction orthogonality, cytocompatibility and efficiency. Specific tasks in this objective were:

- To test whether crosslinking of thiol-norbornene hydrogels can be initiated by HRP in the presence of , with H_2O_2 supplied either directly or indirectly through GOX/glucose reaction (Figure 2.1).
- To examine whether mechanical properties of the enzymatically crosslinked thiol-norbornene hydrogels can be tuned via adjusting HRP, H_2O_2 and macromers concentration or by adjusting thiol/norbornene ratio.
- To evaluate whether the incorporation of tyrosine residue within the sequence of peptide crosslinkers can improve gelation kinetics.
- To stiffen enzymatically crosslink hydrogels via mushroom tyrosinase mediated DOPA-dimer crosslinking and to evaluate the effect of hydrogel stiffening on changes in cell morphology.

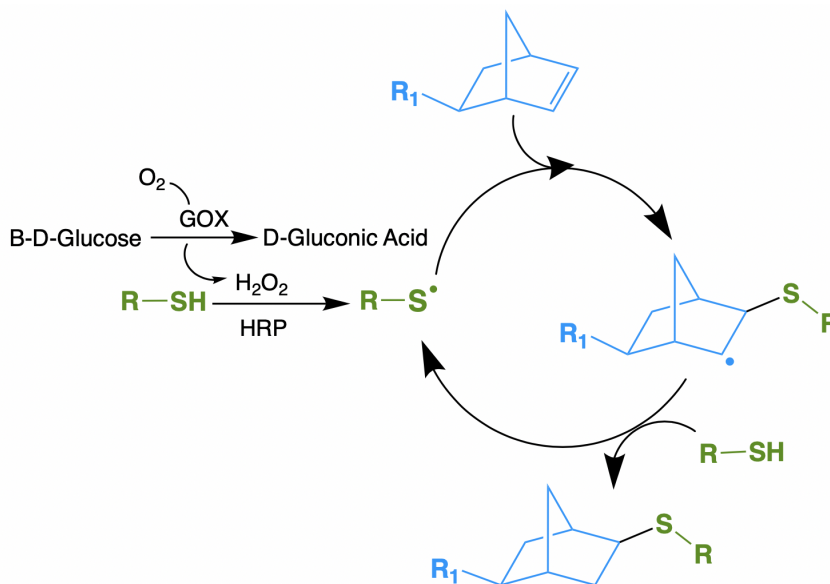


Fig. 2.1: Schematic of HRP-mediated thiol-norbornene polymerization.

2.2 Objective 2: Mushroom Tyrosinase-triggered Boronic acid-DOPA Dynamic Covalent Bonds Formation

The second objective of this thesis was to convert the initially elastic hydrogel to a viscoelastic one via enzymatic reaction. Hydrogels can be made to carry both boronic acid and tyrosine moieties within their network. After treatment of hydrogel with MT and ascorbic acid, the oxidation of tyrosine residues will be stopped at the catechol product, which can immediately click with BA moieties due high binding affinity. The formation of the dynamic covalent bond effectively introduces viscoelasticity to the initial elastic hydrogels (Figure 2.2). The dynamic bond can reorganize and dissipate energy if stress was imposed on it by cells or other sources. The specific tasks were:

- To fabricate gelatin-based hydrogels containing boronic acid (BA) and hydroxyphenyl acetate (HPA).
- To confirm the conversion of HPA to DOPA in the presence of ascorbic acid (AA) and mushroom tyrosinase (MT).

- To examine the viscoelasticity of the hydrogels after treatment with MT and AA.
- To conduct preliminary cell study and observe cell behavior within the converted viscoelastic hydrogel.

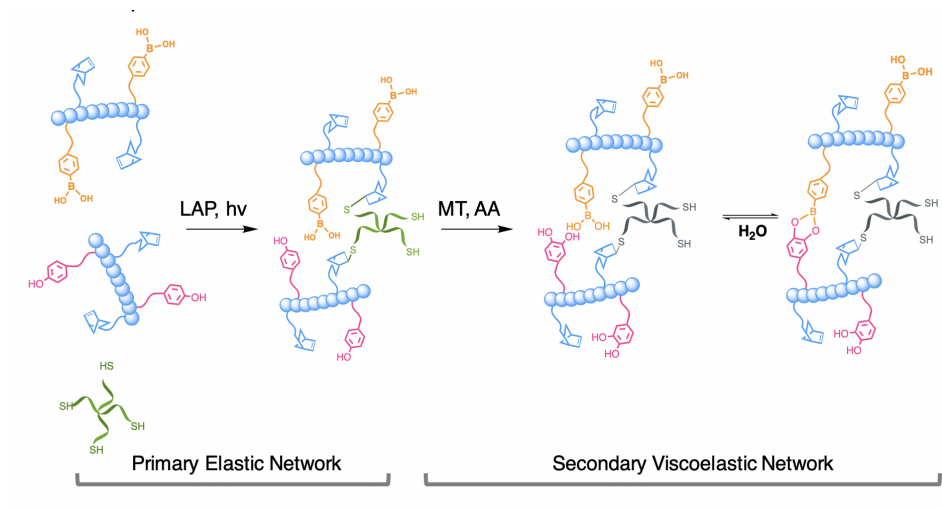


Fig. 2.2: Schematic of mushroom tyrosinase-induced viscoelastic hydrogel.

CHAPTER 3. MATERIALS AND METHODS

3.1 General Materials

8-arm poly(ethylene glycol) (PEG-OH) (20 kDa) was purchased from JenKem Technology; HRP (220 U/mg) and mushroom tyrosinase (MT, 845 U/mg) were purchased from Worthington. GOX (111 U/mg) was acquired from Amresco. All other chemicals were purchased from Fischer Scientific and used without further purification unless otherwise stated. Photoinitiator lithium aryl phosphinate (LAP) were synthesized as described previously [54].

3.2 Macromers Synthesis

Following protocol published previously [23], 8-arm PEG-norbornene was synthesized with minor modifications. Briefly, 5-norbornene-2-carboxylic acid (5-fold molar excess to hydroxyl groups on PEG) was dissolved in anhydrous DCM and reacted with N,N,-dicyclohexylcarbodiimide (DCC) for 1 hour to obtain norbornene anhydride. The norbornene anhydride solution was filtered to remove by-product precipitate urea and added to a flask containing 8-arm PEG-OH, DMAP (0.5 equivalent), and pyridine (0.5 equivalent). The flask was covered, and the reaction was allowed to proceed overnight on ice. The reaction was repeated with additional norbornene anhydride to improve the norbornene substitution. The final PEG8NB product was precipitated in cold ethyl ether, dried in vacuo and redissolved in ddH₂O for dialysis. Dialysis against double distilled water and HCl took place for 3 days before the product was subjected to lyophilization. ¹H NMR (Bruker Advance 500) was used

to confirm the degree of PEG functionalization. PEGNB linear was synthesized in a similar manner. Gelatin-norbornene was synthesized following a published protocol [55], where 10 wt% gelatin (type B) and 20 wt% carbic anhydride were dissolved in DPBS, at 40 °C. The pH value of buffer solution was adjusted to 4.7 with 2N HCl. After 24 hrs, the reaction was quenched by adding 5 times volume of DPBS. Gelatin-norbornene (Gel-NB) product was dialyzed in ddH₂O for 3 days, and lyophilized. The degree of norbornene substitution was determined with fluoraldehyde assay using unmodified gelatin as standard.

3.3 Peptide Synthesis and Purification

All peptides were synthesized using standard solid peptide synthesis in an automated microwave-assisted peptide synthesizer (CEM Liberty 1) using Fmoc-protected amino acids. Peptide cleavage was performed using a cleavage cocktail containing trifluoroacetic acid (TFA), triisopropylsilane (TIS), phenol, and double distilled water with TFA:H₂O:TIS molar ratio equaled 40:1:1 (prepared with 400 mg of phenol, 7.6 ml of TFA, 0.2 ml ddH₂O, and 0.2 ml TIS). The peptides were cleaved from the resin for 3h at room temperature and precipitated in cold ethyl ether, dried in vacuo, purified by reverse phase HPLC (PerkinElmer Flexar system), and characterized with mass spectrometry (Agilent Technologies).

3.4 HRP-mediated Thiol-norbornene Hydrogel Fabrication

To fabricate HRP/H₂O₂ mediated thiol-norbornene hydrogel, macromer PEG8NB was crosslinked with either DTT or bis-cysteine-bearing peptides (i.e. CGGGC, CYGGGYC, CGGYGGC, KCYGGYGGYCK). Specifically, to make a 1:1 thiol to norbornene ($R_{thiol/ene} = 1$) ratio of PEG8NB-KCYGGYGGYCK hydrogel, 3 wt% of PEG8NB and 10 mM of KCYGGYGGYCK (final concentrations) were dissolved in phosphate buffer solution (PBS) at pH 7.4 with 1 U/ml HRP and 0.5 mM H₂O₂. The solution was vortexed for approximately 5 seconds before pipetting in between

two glass slides separated by 1-mm-thick spacers. Gelation occurred within 5 minutes. The hydrogels made with tyrosine-free peptide CGGGC or with DTT and GelNB-PEG4SH gels were also prepared following the same procedure with a more concentrated HRP (100 to 200 U/ml). With HRP/GOX/glucose-mediated gelation, PEG8NB-DTT and PEG8NB-peptide hydrogels were prepared following similar procedure mentioned above. Briefly, 3 wt% PEG8NB and 12 mM (final concentrations) DTT or peptides were dissolved in PBS with 1 U/ml (for tyrosine-containing peptide), or 200 U/ml HRP (for CGGGC and DTT), 1 U/ml GOX, and 10 mM glucose. The solution was vortexed for approximately 5 seconds before pipetting in a Teflon mold with 8-mm diameter cavity. Hydrogel discs were obtained after 10 minutes of gelation. To stiffen hydrogels using MT, PEG8NB hydrogels were crosslinked by tyrosine-containing peptides (CYGGGYC and KYCGGYGGYCK) (thiol to norbornene ratio was fixed at 1). Prior to MT-mediated stiffening, hydrogels were swollen in PBS for 24 hrs to wash off un-crosslinked species. To induce dynamic stiffening, hydrogels were submerged in 1 kU/ml MT for 6 hrs. Afterwards, MT was removed via swelling hydrogels in PBS for 24 hrs. Moduli of the stiffened gels were measured using oscillation rheometry in strain-sweep mode.

3.5 Rheometry

Rheological property measurements were conducted with circular hydrogel discs fabricated between two glass slides. Gel discs were punched out with an 8 mm biopsy punch. The hydrogels were carefully transferred to the rheometer platform prior to initiating the measurements. The shear moduli of hydrogels were determined using a Bohlin CVO 100 digital rheometer fitted with an 8-mm diameter parallel geometry. The measurements were performed in strain-sweep mode with the strain ranging from 0.1% to 5%, and the oscillation frequency was 1 Hz. For in situ gelation experiments, single frequency oscillation test was used (oscillation frequency was 1 Hz and 1% strain). The precursor PEG8NB solution containing thiol crosslinkers, HRP, H₂O₂

(or GOX and glucose) were mixed and vortexed for 5 seconds. Immediately after vortexing, 7 μL of the mixture was placed on the lower plate and the geometry was lowered to 90 μm . A layer of mineral oil was applied on the edge of the plate geometry head to prevent dehydration.

3.6 Norbornene and Thiol Consumption

The thiol conversion study was conducted with precursor solutions containing linear PEGNB, DTT, HRP and H_2O_2 . Portions of the solution was collected immediately after mixing and at intervals of every 2 minutes afterward for Ellman's assay to determine thiol contents. The thiol concentration left at each specific time point was used to determine the amount of thiol that had been consumed. As for norbornene consumption, mixtures of linear PEGNB, DTT, HRP, H_2O_2 at different thiol to norbornene ratios (keeping PEGNB concentration constant at 3.5 wt%), were prepared and subjected to NMR analysis. NMR spectra were recorded on a Bruker Avance III 500 Hz. Polymer samples for ^1H NMR analysis were prepared at a concentration of 20 mg/ml. The amount of norbornene left after the reaction for each $R_{\text{thiol/ene}}$ ratio was calculated using the ratio of the integration of the norbornene peaks at 6.00 to 6.36 ppm over the integration of the PEG backbone region from 4.21 to 4.37 ppm.

3.7 Characterization of Gel Fraction

Hydrogels were formed with PEG8NB, DTT, HRP and H_2O_2 (or GOX/glucose); each gel was prepared from 45 L of precursor solution. Immediately after gelation, hydrogels were dried in vacuo and weighed to obtain first dried weight ($W_{\text{dry},1}$). The dried gels were incubated in dd H_2O at 37 $^\circ\text{C}$ overnight to remove un-crosslinked species. Afterwards, swollen weights were obtained; swollen gels were dried and

weighed again to obtain the second dried weight ($W_{dry,2}$). Gel fraction was determined by the ratio of the second dried weight over the first dried weight:

$$Gel\ fraction = \frac{W_{dry,1}}{W_{dry,2}}$$

Hydrogel mass swelling ratios (Q) were calculated following equation:

$$Q = \frac{W_{swollen}}{W_{dry,2}}$$

3.8 In-gel Oxygen Measurements

A needle-type oxygen probe connected to Microx4 oxygen sensor (PreSens Precision Sensing GmbH) was used to obtain the oxygen concentrations within the gels. The needle of the oxygen probe was inserted into the gel at specified time points. After needle penetration, the optical fiber of the probe was extended to the tip of the needle so that it was exposed to the gel but remained housed within the needle.

3.9 3T3 Fibroblasts Encapsulation

Cytocompatibility of the enzymatically crosslinked thiol-norbornene hydrogels were evaluated using 3T3 fibroblasts. Cells were cultured in high glucose Dulbecco's modified eagle medium (DMEM) containing 10% fetal bovine serum and 1% penicillin-streptomycin before performing cell encapsulation. A solution of 3 wt% PEG8NB, 13 mM KCYGGYGGYCK peptide, 1 mM CRGDS peptide, 1 U/ml HRP, and 0.5 mM H_2O_2 were mixed together then 3T3 cells were gently suspended into precursor solution at a density of 2×10^6 cells/ml. The mixture was then added to syringes with the top cut open and allowed to gel for 5 minutes. After that, cell-laden gels were transferred into a 24-well plate. GelNB-PEG4SH cell-laden hydrogels were prepared following similar steps but with higher HRP concentration (100 U/ml) and no addition of CRGDS peptide. To evaluate cell viability after encapsulation and throughout culturing period, the encapsulated cells were stained with NucBlue, which labels nuclei

of all cells, and NucGreen, which stains cells with compromised plasma membranes (i.e., dead cells). The numbers of live (all cells minus dead cells) and dead cells were imaged with a confocal microscope and counted using ImageJ software.

3.10 Dynamic Stiffening of Enzymatically Crosslinked PEG-peptide Hydrogels

MT was used to induce dynamic stiffening of PEG8NB-peptide hydrogels following procedure mentioned in section 2.3. Briefly, 24 hrs after cell encapsulation, the gels were incubated in 1 kU/ml MT for 6 hours, and the enzyme was removed via swelling in culture media for 24 hrs. To observe the effect of matrix stiffening on cell morphology and cytoskeletal organization, cell-laden hydrogels were fixed and stained for cell nuclei and F-actin. Briefly, at predetermined time after encapsulation, cell-laden hydrogels were fixed with 4% paraformaldehyde and permeabilized with saponin solution following a published protocol. Then, rhodamine phalloidin and DAPI were used to stain for F-actin and nuclei, respectively. Live/Dead and immunofluorescence stained samples were imaged with Olympus Fluoview FV100 laser scanning microscopy. Live/Dead images were captured at 10x objective, with Z-stacked of 10 slices and 10 μm per slice. Immunofluorescence images were captured at 20x objective, with Z-stacked of 10 slices and 2 μm per slice.

3.11 Functionalization of Gelatin with Boronic Acid and Hydroxylphenolic Acid

To further functionalize gelatin-norbornene with boronic acid, 1 g of GelNB (type B) was dissolved in 25 ml of double distilled water at 40 °C. Next, 10 mmol of boronic acid was dissolved in 15 ml of DMF/water mixture at 3:2 ratio, into which 10 mmol of 1-ethyl-3-(3-dimethylaminopropyl) carbodiimide (EDC) and 10 mmol of N-hydroxysulfosuccinimide (NHS) was added. The EDC/NHS reaction was allowed to run for 30 minutes before the gelatin solution was added. The mixture was then

allowed to stir for 48 hours at room temperature. The modified gelatin was dialyzed for 3 days to remove impurities. After dialysis, the functionalized gelatin (GelNB-BA) was frozen, lyophilized at $-50\text{ }^{\circ}\text{C}$, and stored at $-2\text{ }^{\circ}\text{C}$. The functionalization of GelNB with hydroxylphenol acetate (HPA) was proceeded following the same procedure with BA replaced by HPA.

3.12 Mushroom Tyrosinase-triggered Boronic acid DOPA Dynamic Covalent Bonds Formation

MT was also used along with ascorbic acid to generate L-DOPA, which in turn leads to formation of boronic ester dynamic covalent bonds. GelNB-BA, GelNB-HPA, PEG4SH were used to make thiol-norbornene hydrogel via UV-mediated gelation (365 nm, for 2 minute, 1 mM LAP as an initiator). After incubating in PBS for 24 hours to wash off unreacted reagents, GelNB-BA/GelNB-HPA/PEG4SH hydrogels were incubated in 0.5 kU/ml MT and 2.5 mM AA at $37\text{ }^{\circ}\text{C}$. After 6 hours, MT and AA were removed by incubating hydrogels in PBS.

3.13 MBTH colorimetric assay to detect dopachrome formation

To perform MBTH assay, 10 mM soluble tyrosine or GelNB-HPA and 2 mM MBTH reagent were mixed with AA at concentrations ranging from 0.2 mM to 1 mM. After that, 0.2 kU/ml MT were added to the mixture and immediately subjected to absorbance analysis on the micro plate reader at 475 nm.

3.14 BA-conjugated Lucifer Yellow Fluorescent Assay to Detect DOPA-formation

BA was conjugated to lucifer yellow by mixing 2 mmol of 4-amino-3,6-disulfo-1,8-naphthalic anhydride dipotassium salt (lucifer yellow) with 10 mmol 3-aminophenylboronic acid in 1 mL of 5% acetic acid for 2hrs at $60\text{ }^{\circ}\text{C}$ until the solution became clear.

Afterward, the solution was cooled to room temperature and allowed to crystalized overnight at 4 °C. The crystal was collected by centrifuge and washed with ethanol three times. The final product was subjected to NMR analysis. To perform Luc-BA fluorescence assay, soluble GelNB-HPA were prepared at various concentration ranging from 0.03125 mM to 2 mM and mixed with 0.2 mM BA-lucifer yellow, 0.2 U/ml MT, and 5 mM ascorbic acid. The fluorescence was excited at 380 nm and the emission intensity was recorded at 528 nm. The emission was normalized using fluorescence emission of solution containing 0.2 U/ml MT, 5 mM AA, no addition of GelNB-HPA or Luc-BA

CHAPTER 4. RESULTS AND DISCUSSION

4.1 HRP-mediated Thiol-norbornene Hydrogels

4.1.1 Characterization of HRP-mediated Thiol-norbornene gelation

In the past, myriad of hydrogel networks formed via HRP has been reported. In this project, HRP is used to prepare thiol-norbornene hydrogels that are crosslinked traditionally by photopolymerization. We hypothesized that in the presence of H_2O_2 , HRP was activated to become a powerful oxidant that can generate active thiyl radicals. These thiyl radicals can propagate to the norbornene groups, creating carbon-center radicals to continue abstracting hydrogens from other thiols, eventually forming stable thioether bonds. Enzymatic hydrogel formation was confirmed with both a simple tilt test and in situ rheological analysis. As seen in Fig 4.1, gelation only occurred when all components, including PEG8NB macromers, crosslinker DTT, HRP, and H_2O_2 were present.



Fig. 4.1: Tilt test of HRP-mediated thiol-norbornene hydrogel. All components: 200 U/mL HRP, 0.5 mM H_2O_2 , 3.5 wt% PEG8NB, and 14 mM DTT.

In the absence of any one component, hydrogel did not form, indicating thiol-norbornene indeed was triggered by HRP/ H_2O_2 reaction. Moreover, solution with only PEG4SH macromer (i.e., No PEG8NB (+PEG4SH) group) did not yield hydrogel within 30 minutes, indicating hydrogel was not crosslinked by HRP-mediated disulfide bond formation.

In situ rheology was conducted to determine gelation kinetics of the enzymatic reaction, where the time of G'/G'' crossover was defined as gel point. At 200 U/ml HRP and 0.5 mM H_2O_2 , gelation occurred rapidly within 80 seconds (Figure 4.2), with kinetics comparable to that of light-mediated thiol-norbornene hydrogels [23].

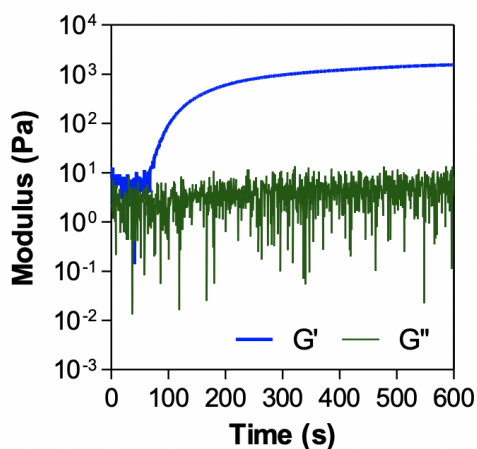


Fig. 4.2: In situ rheometry of HRP-initiated thiol-norbornene gelation (3.5 wt% PEG8NB, 14 mM DTT, 200 U/ml HRP, 0.5 mM H_2O_2).

Next, thiol and norbornene conversion experiments were conducted to further confirm that gelation indeed occurred via HRP-mediated thiol-norbornene reaction. For these experiments, linear PEG was used to allow solution-based assay and to prevent hydrogel crosslinking. Via quantifying free thiol contents within the precursor solution overtime, thiol depletion kinetics can be generated. As shown in Figure 4.3 A, complete conversion of thiol was achieved only in the presence of HRP, H_2O_2 and PEGNB. Without PEGNB addition, only 40% of thiol was consumed, potentially

due to HRP-mediated disulfide formation. As for norbornene conversion, solutions of PEGNB, DTT, HRP and H_2O_2 at different thiol to norbornene ratios were prepared and subjected to proton NMR to analyze chemical shift of the norbornene functional groups. As the thioether bonds formed, disappearance of norbornene peak was observed. The NMR result showed linear relationship between thiol-norbornene ratio and norbornene consumption (Figure 4.3 B), which is one unique feature of orthogonal reactions.

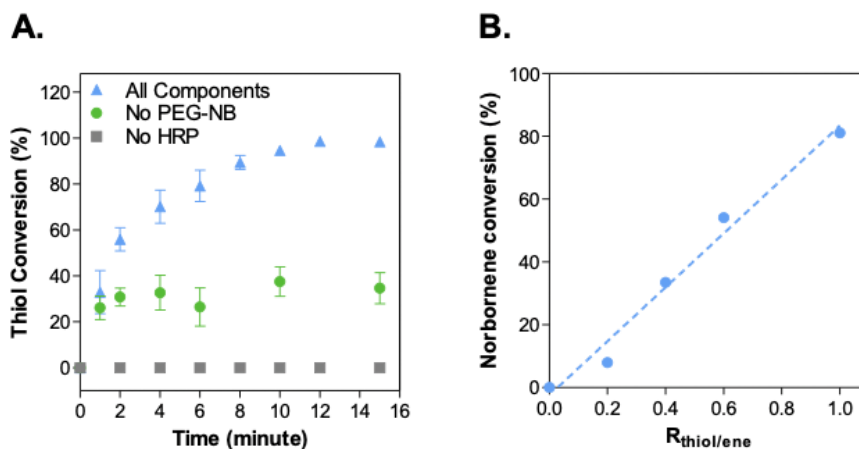


Fig. 4.3: (A) Thiol conversion profiles as a function of reaction time. (B) Norbornene conversion as a function of thiol-norbornene ratio.

To optimize gelation conditions, hydrogels were prepared at various concentrations of HRP and H_2O_2 . As seen in Fig 4.4 A and B, gelation can be achieved at relatively low HRP and H_2O_2 concentrations. Within 10 minutes gelation time, increase in HRP concentration resulted in higher moduli. Similarly, adding more H_2O_2 also improved crosslinking density. Both trends were consistent with earlier literature [9]. Through adjusting PEG8NB content, we showed that hydrogel properties can be readily tuned to obtain moduli relevant to many normal and diseased tissues (1000 - 3000 Pa) including stem cells differentiation [56–58], wound healing [5], tumor progression [2, 7, 44].

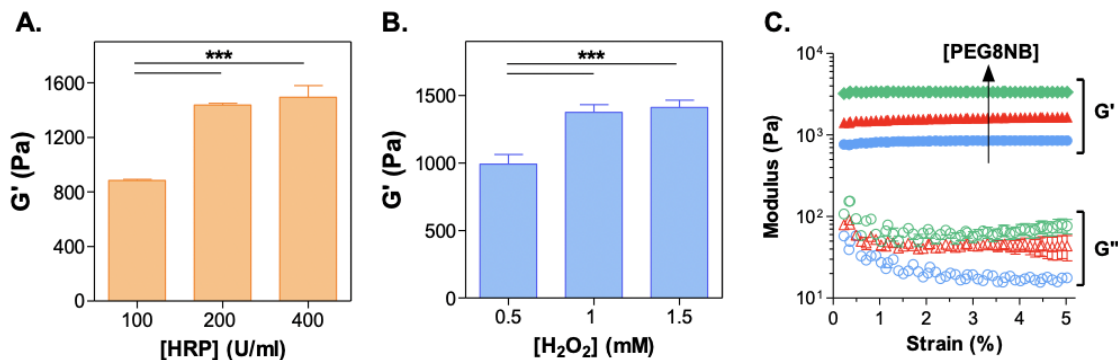


Fig. 4.4: Effect of (A) HRP concentrations and (B) H_2O_2 concentration on shear moduli of PEG8NB-DTT hydrogels. Gelation was formed with 3.5 wt% PEG8NB, and 14 mM DTT, $R_{thiol/ene}=1$. $N = 3$, mean \pm SEM). (C) Strain-sweep rheometry of thiol-norbornene hydrogels formed with different macromer contents (3, 3.5, and 4 wt%. $R_{thiol/ene} = 1$). ($n \geq 3$, Mean \pm SEM, *** $p < 0.001$).

In principle, the enzymatic crosslinking can be adapted for injectable delivery of thiol-norbornene hydrogel that possesses the shape and size of delivery site without limitation of light attenuation. Figure 4.5 showed that unlike photopolymerization, HRP-catalyzed thiol-norbornene hydrogel could form homogeneously throughout large thickness and maintain the integrity of the syringe mold.



Fig. 4.5: HRP-crosslinked thiol-norbornene hydrogel with a diameter of 4 mm and a length of 15 mm (200 U/mL HRP, 0.5 mM H_2O_2 , 3.5 wt% PEG8NB, and 14 mM DTT).

4.1.2 Tyrosine-assisted enzymatic crosslinking of PEG-peptide hydrogels

After demonstrating the feasibility of HRP-initiated thiol-norbornene hydrogel crosslinking using DTT as a cross-linker, we utilized bis-cysteine peptide linkers to form PEG-peptide hydrogels as peptide linkers are advantageous in tissue engineering applications. First, a model peptide linker containing only terminal cysteines and internal glycine residues (i.e., CGGGC) was used for gelation with PEG8NB under 1 mM H_2O_2 and a range of HRP concentrations (i.e., 1 to 200 U/mL). While gelation occurred at high HRP concentrations (100-200 U/mL) as expected, no sol-gel transition was observed when HRP concentration was lower to 5 U/mL even after 30 minutes (data not shown). In an attempt to lower HRP concentration to be more on par with other reported HRP-triggered hydrogel systems, we examined whether adding soluble tyrosine could promote HRP-mediated thiol-norbornene gelation. This approach was reported to improve HRP-induced crosslinking of thiolated polymer [59], as well as the gelation efficiency of photopolymerized thiol-norbornene hydrogels [60].

Unfortunately, soluble tyrosine also did not improve PEG8NB-CGGGC gelation, no gel was observed at 5 U/mL HRP (data not shown). Utilizing information reported by Mishina et al., where tyrosine/cysteine dually labeled protein can be used to facilitate HRP-mediated disulfide crosslinks, we designed peptide sequences containing both cysteine and tyrosine residues, with tyrosine placed directly next to cysteine (CYGGGYC and KCYGGYGGYCK) [61]. Surprisingly, with these new peptides, immediate gelation was obtained at 5 U/mL HRP and 1 mM H_2O_2 , suggesting that close proximity between cysteines and tyrosine residues improved thiol radical generation, hence thiol-norbornene gelation. We hypothesized that hydroxyl phenol radicals were generated on the tyrosine residues first, then rapidly transferred to cysteines within the same sequence, subsequently initiating thiol-norbornene reaction (Figure 4.6) [62], [63]. Because HRP substrate binding site contains mostly hydrophobic residues [64], [65], tyrosine residues fit better than cysteine within HRP pockets in tyrosine-containing peptide chains, the radical generation rate was higher, leading to fast gelation. A control test was performed where PEG8NB and KGYGGYGGYCK (containing no cysteine) peptide used to make hydrogel clarified that gelation was not due to norbornene-tyrosine reaction.

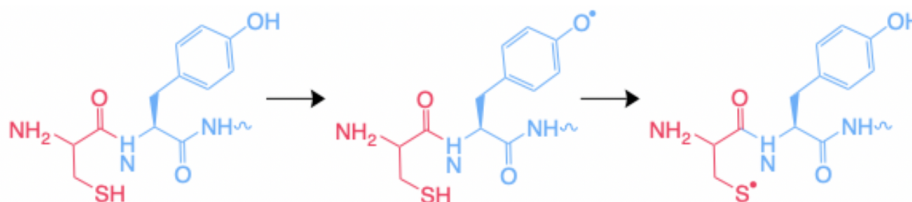


Fig. 4.6: Proposed schematic of thiol radical generation via tyrosine residues.

In order to obtain hydrogel in a more manageable timeframe, concentration of HRP was intentionally lowered H_2O_2 to 1 U/mL and 0.5 mM, respectively for PEG8NB-KCYGGYGGYCK/CYGGGYC hydrogels. Between the two tyrosine containing peptides, the degree of crosslinking was higher when using peptide with higher tyrosine

content (Figure 4.7 A), further proving that tyrosine enhanced gelation efficiency. By varying thiol to norbornene ratio, the moduli of hydrogel can be tuned providing additional means to control hydrogel properties (Figure 4.7 B).

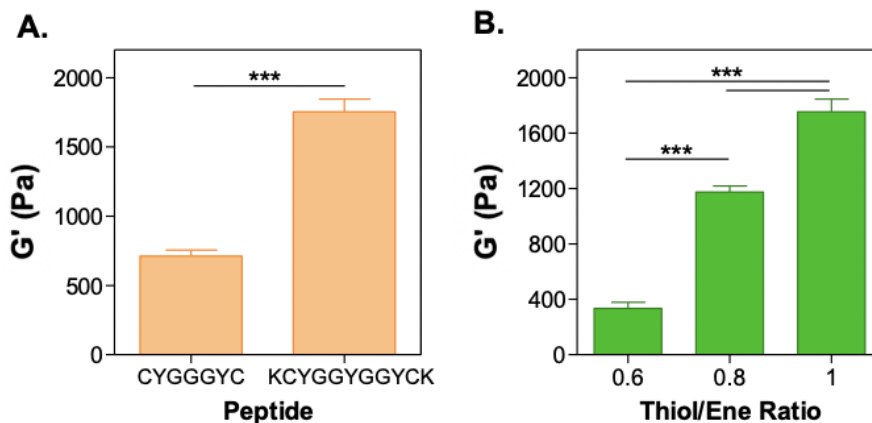


Fig. 4.7: Effect of (B) tyrosine concentration and (C) thiol to norbornene ratios on the shear moduli of hydrogels. Hydrogels were crosslinked at 1 U/ml HRP, 0.5 mM H_2O_2 ($n=3$, Mean \pm SEM, *** $p < 0.001$).

4.1.3 HRP/GOX Dual Enzymatic Thiol-norbornene Gelation

As the initial excess H_2O_2 is known to impede HRP reactivity [66], [67] the use of exogenous H_2O_2 are typically undesirable in biomedical applications, we utilized GOX and glucose to supply H_2O_2 in situ for the activation of HRP. This method supposedly increases the efficiency of the HRP-mediated gelation system by supplying larger amount of H_2O_2 overtime with less initial inactivation of HRP [68]. Schematic of the reaction incorporating GOX/glucose is shown in Figure 1.4. Gelation occurred when GOX, glucose, dissolved oxygen and HRP were present with no exogenous H_2O_2 needed. Similar to the HRP/ H_2O_2 system, HRP/GOX gelation were highly controllable. By varying glucose concentrations, the moduli of the hydrogels fabricated with PEG8NB and CYGGGYC can be tuned almost linearly using 1 to 10 mM glucose

at 10 U/ml GOX and 1 U/ml HRP (Figure 4.8 A). However, at 15 mM glucose concentration, the hydrogel moduli started to decline, supposedly due to the excessive H_2O_2 amount generated that undermined HRP or GOX activity [42, 43].

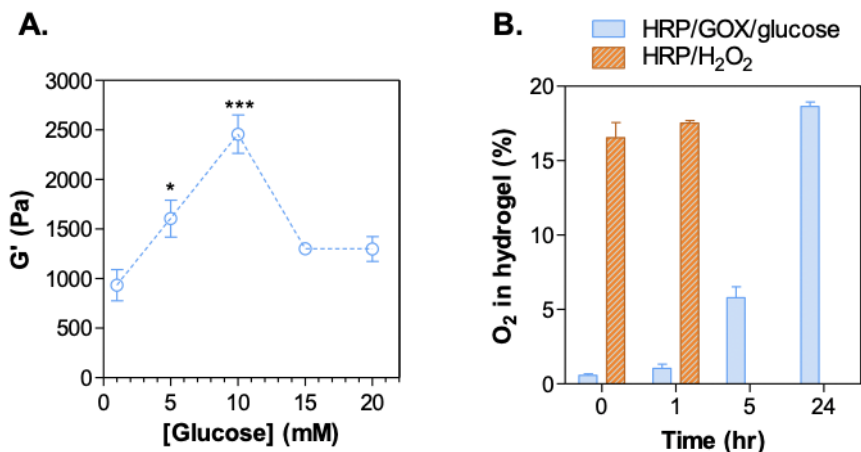


Fig. 4.8: (A) Effect of glucose concentrations on shear moduli of dual enzyme-crosslinked thiol-norbornene hydrogels (1 U/mL HRP, 10 U/ml GOX, 3 wt% PEG8NB, and 12 mM CYGGGYC, $R_{thiol/ene} = 1$). (B) Oxygen contents within hydrogels formed by HRP/GOX/glucose (1 U/ml HRP, 1 U/mL GOX, 10 mM glucose) and HRP/ H_2O_2 (1 U/mL HRP, 0.5 mM H_2O_2).

Because the GOX/glucose reaction consumes oxygen to generate H_2O_2 , effect of the dual enzymes reaction on oxygen contents was investigated. We used a needle-type oxygen probe to detect concentrations of dissolved oxygen inside two groups of hydrogels HRP/ H_2O_2 and HRP/GOX at various time points post-gelation (0-24 hrs). Hydrogels were made and placed in PBS immediately after gelation. As shown in Figure 4.8 B, oxygen contents inside the hydrogels formed by HRP/ H_2O_2 -initiated gelation remained close to normoxia after gelation as no dissolved oxygen was needed in HRP/ H_2O_2 -mediated reaction. However, in the HRP/GOX/glucose gelation system, hypoxia ($\sim 1\%$) was detected within an hour post-gelation. After 5 hours, O_2 content started to slowly regain to 6%. Oxygen level in the hydrogel

returned to almost normoxia after 24 hours, presumably due to oxygen diffusion into the gel overtime. The increased 'in-gel oxygen' results also demonstrated that no GOX/glucose reaction were taken place within hydrogel 24 hrs after after crosslinking. By this point, most of the glucose have either been consumed or diffused out of the matrix. Similarly, GOX was no longer present within hydrogels.

We further compared gel fraction, mass swelling ratio, and storage moduli (G') of the two HRP-initiated thiol-norbornene hydrogels to that of UV crosslinked gels with the same macromer compositions. Figure 4.9A shows that gel fractions of hydrogels crosslinked by the HRP/GOX/glucose system (87.4 ± 2.08) were comparable to that of UV crosslinked gels (87.8 ± 2.43), suggesting high crosslinking efficiency of the enzymatic thiol-norbornene reactions. The HRP/ H_2O_2 system showed slightly lower gel fraction (77.5 ± 0.98), likely due to partial inactivation of HRP by exogenously added H_2O_2 that reduced the efficiency of the crosslinking reaction [67,69]. Mass swelling ratio and G' also followed the same trend indicating HRP/GOX produced more effective crosslinking than HRP/ H_2O_2 system does. Higher moduli can be obtained using the UV light-mediated and HRP/GOX systems.

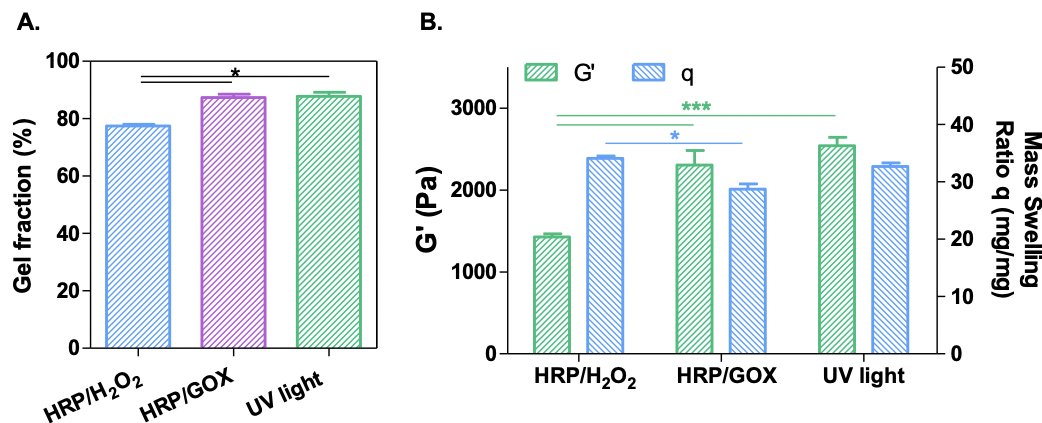


Fig. 4.9: (A) Gel fraction (B) Mass swelling ratio and Storage Moduli G' of hydrogels formed with HRP/H₂O₂, HRP/GOX and UV light-mediated thiol-ene photopolymerization. (3.5 wt% PEG8NB-DTT, $R_{thiol/norbornene} = 1$, $n = 3$, mean \pm SEM, * $p < 0.05$). HRP/H₂O₂ gels were formed with 200 U/ml HRP and 1 mM H₂O₂; HRP/GOX gels were formed with 200 U/ml HRP, 10 U/ml GOX, and 10 mM glucose. UV light-mediated gels were formed with 1 mM LAP, and UV light at 365 nm wavelength for 2 minutes.

4.1.4 Enzymatically Crosslinking of Gelatin-based Thiol-norbornene Hydrogels

To demonstrate versatility of the enzymatic gelation system, gelatin functionalized with norbornene group (GelNB) was used with PEG4SH to fabricate hydrogels. Gelatin possesses intrinsic biodegradability and biocompatibility that are desirable in tissue engineering. Both H₂O₂ and GOX/glucose can be used to induced HRP-mediated gelation. As expected, similar to the PEG-based hydrogel, the GelNB-PEG4SH hydrogel could be made and readily tuned through adjusting either gelatin content (Figure 4.10A) or thiol to norbornene ratio (Figure 4.10B). Higher crosslinking density can be obtained using higher macromer concentration or by us-

ing thiol/norbornene ratio closer to one. It is worth noting that, both GelNB and PEG4SH are multifunctional macromers. Therefore, HRP concentration were lowered to 100 U/ml to achieve slower gelation time and allowing more homogenous mixing.

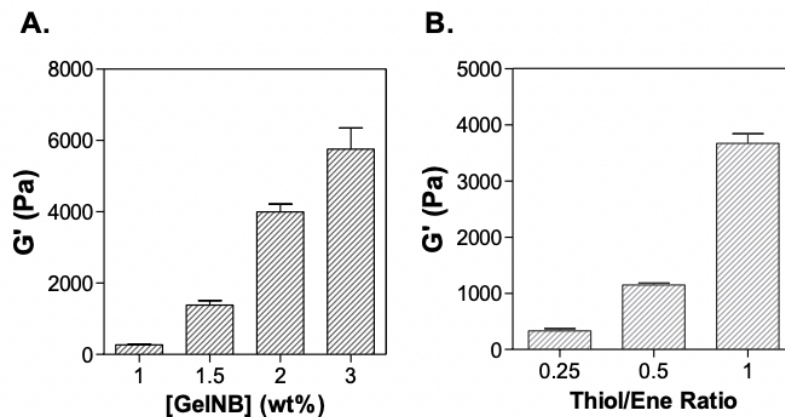


Fig. 4.10: Effect of gelatin content (A) and thiol to norbornene ratio (B) on the moduli of GelNB-PEG4SH hydrogels (100 U/ml HRP, 10 U/ml GOX, 10 mM glucose) ($n \geq 3$, Mean \pm SEM, * $p < 0.05$, *** $p < 0.001$).

4.1.5 Dynamic Stiffening of Enzymatically Crosslinked PEG-peptide Hydrogels

To ascertain our hypothesis that tyrosine transferred its radicals to thiol groups and regain its hydrogen after hydrogel formation, we subjected PEG8NB-CYGGGYC (2Y) and KCYGGYGGYCK (3Y) hydrogels to mushroom tyrosinase (MT)-mediated stiffening. MT oxidizes the tyrosine residues into DOPA, and eventually DOPA dimer, forming a secondary network and stiffens the hydrogel (Figure 4.11 A). As seen in Figure 4.11 B, MT successfully oxidized tyrosine into DOPA-dimer, shrunk the hydrogel slightly and changed the color of hydrogel from transparent to dark brown, a characteristic color of MT-catalyzed DOPA products [70–72]. The stiffening occurred in hydrogels crosslinked by peptides with two or three tyrosine residues, as well as gels crosslinked with HRP/H₂O₂ or HRP/GOX/glucose systems. The result

confirmed that the hydroxyl-phenol groups on tyrosine remained protonated following HRP-mediated gelation. Most importantly, the degrees of stiffening were relevant to normal and pathological tissue mechanics [5].

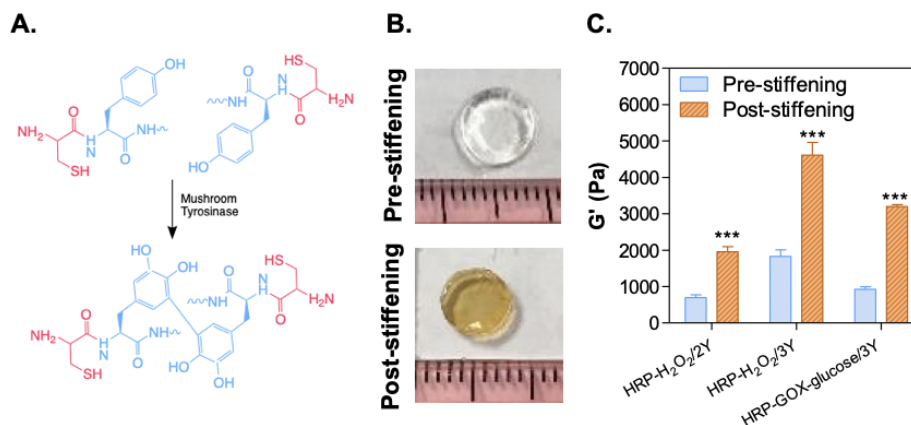


Fig. 4.11: (A) Schematic of MT-induced post-gelation dynamic crosslinking. (B) Photographs of enzymatically crosslinked PEG-peptide (2.5 wt% PEG8NB and KCYGGYGGYCK (3Y) thiol-norbornene hydrogels pre- and post-stiffening. Gel crosslinking was initiated by 1 U/mL HRP, 10 U/mL GOX, and 10mM glucose. Stiffening was induced by incubating the swollen gels in PBS containing 1 kU/mL MT. (C) Shear moduli of hydrogels pre- and post-stiffening. HRP = 1 U/ml, HRP/ H_2O_2 hydrogels were made with 3 wt% PEG8NB, while HRP/GOX-glucose were made with 2.5 wt% PEG8NB to give modulus around 1000 Pa. (n=3, Mean \pm SEM, *** $p < 0.001$).

4.1.6 Cell Encapsulation and Dynamic Stiffening of Cell-laden Hydrogels

To test the cytocompatibility of HRP system, 3T3 fibroblast was used for encapsulation. It has been shown that GOX/glucose system were more ideal for cell encapsulation because H_2O_2 can be consumed immediately by HRP as it is generated.

Ideally, this can ameliorate the toxic effect of adding a large amount of H_2O_2 [36]. However, the in-gel extreme hypoxia observed in Figure 4.8 B might not be ideal for cell culture. Another potential challenge with the HRP/GOX/glucose system as a means to supply H_2O_2 includes the continuous consumption of glucose within the culture media by GOX. Therefore, HRP- H_2O_2 system was used in this thesis for cell encapsulation studies.

For cell encapsulation application, a very low concentration of H_2O_2 was used (0.5 mM), which can be consumed within seconds by HRP, permitting minimal toxicity to cells. As Live/Dead staining indicated in Figure 4.12A, 85% cells encapsulated within GelNB-PEG4SH were alive 24 hrs after encapsulation. DAPI and F-actin staining shown in Figure 3.12B revealed significant cell spreading and proliferation after 8 days of culturing, indicating the encapsulated cells were able to attach to gelatin network as well as degrade the matrix through protease and form interconnected cell network.

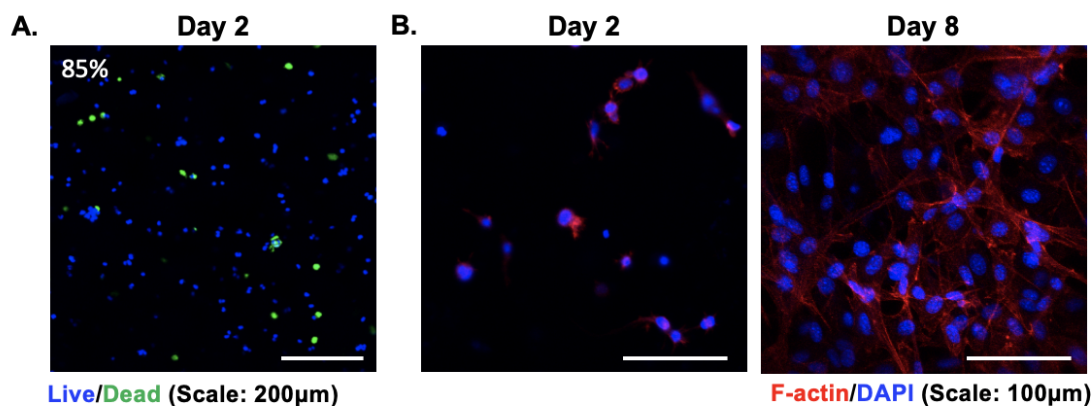


Fig. 4.12: (A) Live/Dead staining images of 3T3 cultured in GelNB-PEG4SH hydrogels 24 hrs after encapsulation. Hydrogels were formed with 1.5 wt% GelNB-PEG4SH, 100 U/ml HRP, and 0.5 mM H_2O_2 , modulus $G' = 1000$ Pa. (B) Fluorescence staining images of spread 3T3 at day 1 and day 8.

Next, using PEG8NB and peptides containing tyrosine residues, the effect of matrix stiffening on cell fate was investigated. After cells were encapsulated within PEG8NB-KCYGGYGGYCK gels, the gels were split into 2 groups, one group received MT treatment (stiffened group), the other was left in regular culture media (soft group). One day after the treatment took place, no significant cell death occurred as revealed by live/dead staining and the cells remained viable through the whole culturing period (Figure 4.13). To observe changes in cell morphology, fluorescent staining of the nuclei and cell cytoskeleton was used. Although no difference was observed in cell morphology 24 hrs after MT treatment, after 8 days, cells within soft gels had spread significantly with dramatic interconnect cell network while cells encapsulated within stiffened hydrogels had only started to develop minimal protrusion. The smaller mesh size in stiffened hydrogels was hypothesized to restrict cell motility and to limit their spreading, resulting in rounded single cells. Stiffening did not decline cell proliferation as live/dead staining at day 8 showed similar cell density in both soft and stiff groups. It is also worth noting that the hydrogels crosslinked by PEG8NB-peptide exhibited higher cell viability comparing with gels formed by GelNB-PEG4SH. This was likely caused by the use of different HRP concentrations in the two group of gels (i.e., 1 U/ml and 100 U/ml for PEG8NB and GelNB gels, respectively). Potentially, the difference in radical generation between crosslinking with and without tyrosine residue, also affected cell viability. With that said, both PEG-based and gelatin-based system were still appeared to be highly cytocompatible and effective in promoting cell spreading as well as proliferation.

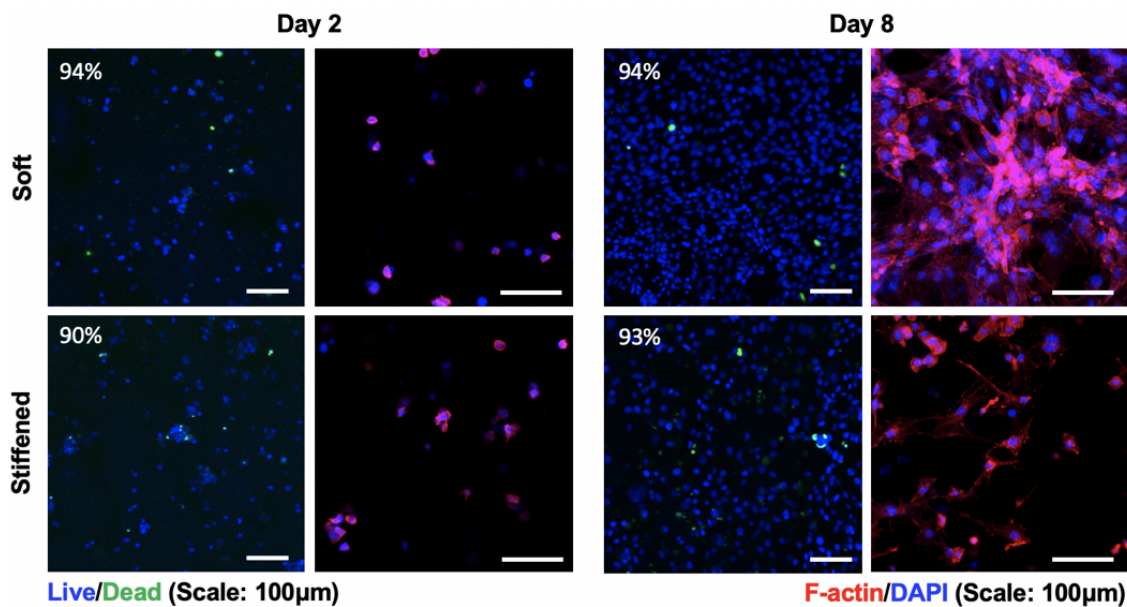


Fig. 4.13: Live/Dead and Fluorescence images of 3T3 at Day 2 (24 hours after stiffening) and Day 8. Stiffened group were treated with 1 kU/ml tyrosinase for 6 hours on day 1. Hydrogels were made with 3 wt% PEG8NB-KCYGGYGGYCK, 1 U/ml HRP, 0.5 mM H₂O₂, $G' \sim 1500$ Pa.

4.2 MT-mediated Viscoelastic Hydrogel Boronic Acid

To further tune the mechanical properties of hydrogel, we developed a hydrogel system that can potentially become viscoelastic with treatment of mushroom tyrosinase and ascorbic acid. Specifically, gelatin macromers containing HPA and BA were synthesized and crosslinked into hydrogels. In the presence of AA, MT triggered formation of DOPA to complex with BA, creating a secondary viscoelastic network within the primary elastic thiol-norbornene hydrogel.

4.2.1 Controlled Formation of L-DOPA Product using MT and Ascorbic acid

To introduce viscoelasticity to hydrogel network, we first need to control the products of MT oxidation to specifically be DOPA, which can then complex with BA. Ascorbic acid has been reported increase specificity of DOPA production via MT by preventing further oxidization of DOPA by MT into dopaquinone and dopachrome. To confirm this, we utilized 3-methyl-2-benzothiazoninone hydrazine (MBTH) to detect dopaquinone and dopachrome formation in the presence of MT at various concentrations of ascorbic acid. The colorless MBTH reacts with ketone functional group on dopachrome to produce a pink pigment that can be detected at 475 nm. As shown in Figure 4.14, increasing AA concentration clearly decreased absorbance at 475 nm, suggesting a delay in the formation of dopachrome caused by AA.

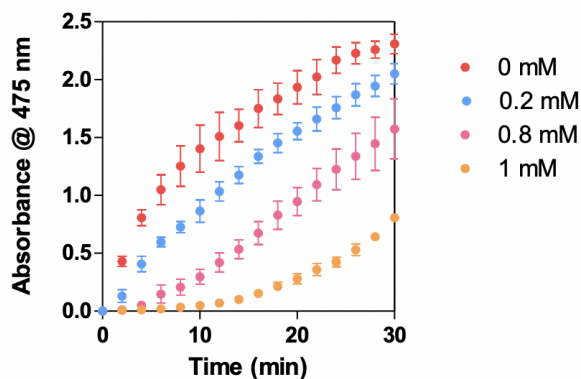


Fig. 4.14: MBTH assay to detect dopachrome formation in the presence of MT and AA. Solution containing 10 mM tyrosine, 0.2 U/ml MT, 2 mM MBTH and various concentration of AA was used.

After confirming that AA delayed dopachrome formation, we utilized fluorescent molecule lucifer yellow conjugated with boronic acid (Luc-BA) to examine whether the delay in dopachrome formation was indeed cause by DOPA generation. When DOPA comes in contact with Luc-BA, the fluorescent intensity will decrease as reported by

Coskun and Akkaya (Figure 4.15 A) [73]. As seen in Fig 4.15 C, in the presence of both MT and AA, GelNB-HPA supposedly formed Gel-DOPA, which complexed with Luc-BA and decreased its emission intensity. On the other hand, the decrease in intensity was not observed within group treated with only AA (without MT), proving that no DOPA was formed in this group. Even though AA is a type of sugar molecule, which can complex with Luc-BA, the affinity of AA and BA was very low (at 16 M^{-1}) [53], hence no significant decrease in emission was detected. Gel-DOPA formed via MT and AA reaction decreased the intensity of Luc-BA to a similar extend with dopamine ($\sim 85\%$ at 1 mM) (Figure 4.15 B), which further confirmed that we had successfully controlled the oxidation of HPA to specifically produce DOPA.

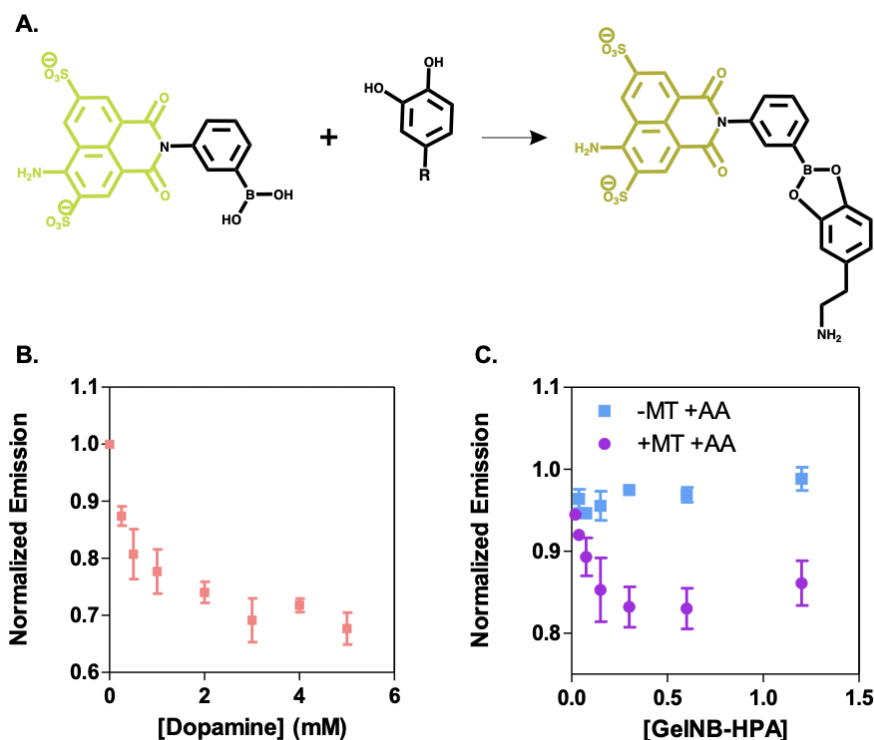


Fig. 4.15: (A) Selective recognition of DOPA by Luc-BA fluorescent molecule. (B-C) Normalized emission intensity of Luc-BA at different concentration of (B) Dopamine and (C) GelNB-HPA in the presence of MT, AA. Excitation wavelength is 430 nm.

4.2.2 Characterization of Primary Elastic Network

Next, using GelNB-HPA and GelNB-BA, we fabricated elastic hydrogel via UV-light mediated thiol-norbornene chemistry with PEG4SH as crosslinkers. Figure 4.17 demonstrated the storage moduli (G') of GelNB-BA/GelNB-HPA/PEG4SH hydrogels at different thiol-norbornene ratio. The elastic modulus of the hydrogels increased as the thiol/norbornene ratio. The newly fabricated gelatin-based hydrogel were immobilized both BA and HPA moieties.

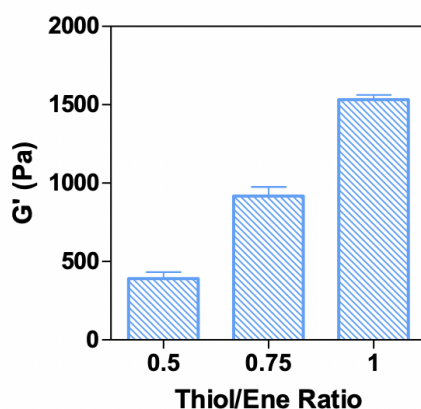


Fig. 4.16: 3 wt% GelNB-BA/3 wt% GelNB-HPA/PEG4SH hydrogels formed via LAP and UV-light (365 nm, 2 minutes) at different thiol-norbornene ratios.

4.2.3 Tunable Viscoelastic Hydrogels via MT and AA

As confirmed in earlier experiments, AA inhibited formation of dopaquinone and dopachrome. We hypothesized that AA would also reduce MT-mediated gelation stiffening. To test this hypothesis, we prepared UV-mediated GelNB-HPA and GelNB-BA/GelNB-HPA hydrogels with PEG4SH as crosslinker, then submerged them in a solution containing 1 kU/ml and 5 mM AA. As was anticipated, hydrogels treated with only 1 kU/ml MT and no addition of AA, stiffened with 3-fold increase in stiffness (Figure 4.18). GelNB-HPA and GelNB-HPA/GelNB-BA hydrogels stiffened to

similar extent, suggesting that incorporating BA moieties within the hydrogel did not interfere with MT-mediated stiffening. On the other hand, in the presence of AA, stiffening did not occur, no change in storage moduli G' was seen after the treatment. Furthermore, the hydrogels did not change their color to dark brown after MT treatment, suggesting that no DOPA dimers were formed and that it was likely that the oxidation of HPA was stopped at the DOPA step.

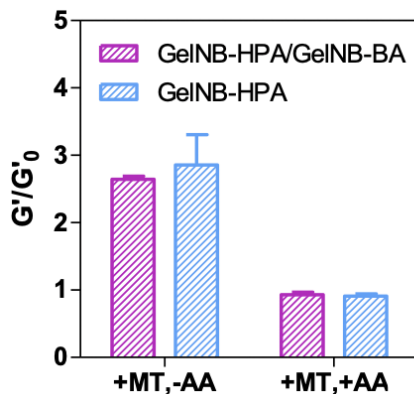


Fig. 4.17: Effect of AA on MT-mediated stiffening. Hydrogels were made from 3 wt% GelNBHPA/3 wt% GelNB-BA/PEG4SH ($R_{thiol/nor} = 0.75$). Hydrogels were incubated in 1 kU/ml MT for 6 hours in the presence and absence of 5 mM AA.

After asserting that Gel-HPA could be converted in to Gel-DOPA using MT and AA, GelNB-BA/GelNB-HPA/PEG4SH hydrogels were made and subjected to treatment with MT and AA to form viscoelastic gels (Figure 1.5). Figure 4.19 A showed that comparing to the control group (no MT), MT treatment of hydrogels led to increase in both G' and G'' , a result of stiffening. Treatment of hydrogels with MT and AA increased G'' , however, G' maintained at the same modulus. The $\tan(\delta)$ was calculated using G''/G' to determine the damping characteristic of the hydrogels. The higher $\tan(\delta)$ value indicates a more viscoelastic material that are capable of dissipate more energy when mechanical force was applied. $\tan(\delta)$ was the highest within the group treated with MT, AA, implying that the hydrogels in this group were the most viscoelastic due to formation of BA-DOPA dynamic bonds. The $\tan(\delta)$ of hydrogels

treated with only MT also had increased $\tan(\delta)$ comparing to the control group, implying the formation of dynamic bonds. It can be hypothesized that even without AA, some DOPA still formed via MT and complex with BA, however without AA most DOPA was converted into DOPA-dimer, resulting in stiffening. Cell encapsulation with the viscoelastic hydrogel needs to be conducted to investigate whether the increase in viscoelasticity was sufficient to impact cells behaviors.

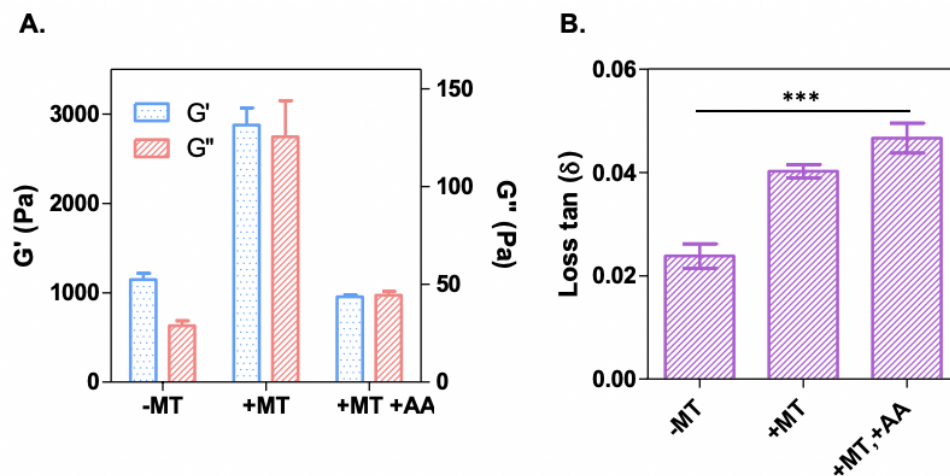


Fig. 4.18: (A) Storage moduli and loss moduli (B) $\tan(\delta)$ of 3 wt% GelNB-BA/3wt% GelNB-HPA/PEG4SH hydrogels ($R_{thiol/norbornene} = 0.75$) treated with no MT; 1 kU/ml MT; and both 1 kU/ml MT, 5 mM AA.

CHAPTER 5. SUMMARY AND RECOMMENDATIONS

5.1 Summary

In summary, an innovative enzymatic method to crosslink orthogonal thiol-norbornene hydrogel was developed. The HRP-mediated system offers researchers an attractive alternative to form in situ thiol-norbornene hydrogel with high controllability and without the concern of light attenuation or UV-light irradiation. The unique features of this hydrogel system include the use of low concentrations of enzyme (both HRP and GOX) and H_2O_2 . More importantly, the preservation of tyrosine residues following the primary thiol-norbornene crosslinking allowed dynamic stiffening of hydrogels via tyrosinase-mediated crosslinking. These available tyrosine residues can also be used as sites for bioconjugation to provide additional biochemical cues within the ECM, if desired. HRP-mediated hydrogel was shown to support survival and proliferation of encapsulated cells. In the second objective of this project, in addition to the on-demand stiffening, MT was used to increase viscoelasticity of an otherwise elastic hydrogel network. This was achieved via generation of DOPA-boronic acid dynamic bonds. It was established that in the presence of MT and AA, the hydroxyl phenol groups off GelNB-HPA chain can be oxidized into GelNB-DOPA. The DOPA moieties complexed with BA moieties within the hydrogel to form a secondary network increasing the network viscoelasticity.

5.2 Recommendations

Although many aspects of HRP-mediated crosslinking system have been carefully investigated, the polymerization kinetics of HRP comparing to UV-light mediated has not been studied, especially in the case involving dual enzymes HRP and GOX. To be used for injectable application, the kinetics of the enzyme-triggered thiol-norbornene reaction is critical data to be collected. In the GOX/HRP system, the gradual release of H_2O_2 can be useful in several tissue engineering applications as reactive oxygen species are implicated to play an important role in wound healing as well as angiogenesis [74]. To mitigate the extreme hypoxic environment caused by GOX/glucose reaction, catalase, an enzyme decomposing H_2O_2 into H_2O and O_2 can be used to supply oxygen within the hydrogels after cell encapsulation. As for the viscoelastic hydrogel system, the effect of viscoelasticity on cellular behavior needs to be investigated. The synergistic effect of viscoelasticity and stiffening via MT could be an interesting aspect to explore. Further treatment of MT in viscoelastic hydrogels should be conducted to see whether stiffening would affect the dynamic boronic ester bonds and how the combined changes in elasticity and viscoelasticity would affect cell behaviors. Furthermore, instead of using only gelatin-based macromers for fabrication of hydrogel, hyaluronic acid (HA) can be incorporated with hydrogel network as a bioactive molecule. HA is a naturally occurring glycosaminoglycan (GAG) and a major component of the native ECM, addition of HA within viscoelastic gel might be beneficial as it would better mimic the heterogeneity of ECM and can increase cell-matrix interaction. HA also processes multiple functional groups along its backbone (carboxylic and hydroxyl groups) that are accessible for dual functionalizations. Lastly, different BA molecules has been reported to obtain different pKa values that could affect the stability of the BA-DOPA complex [52]. Other than the 3-carboxyphenyl boronic acid used in this thesis, different BA molecules with lower pKa should be used to improve the complex stability at physiological pH and increase the viscoelasticity of the network.

LIST OF REFERENCES

LIST OF REFERENCES

- [1] A. D. Theocharis, S. S. Skandalis, C. Gialeli, and N. K. Karamanos, “Extracellular matrix structure,” *Advanced drug delivery reviews*, vol. 97, pp. 4–27, 2016. [Online]. Available: <http://dx.doi.org/10.1016/j.addr.2015.11.001>
- [2] I. Acerbi, L. Cassereau, I. Dean, Q. Shi, A. Au, C. Park, Y. Y. Chen, J. Liphardt, E. S. Hwang, and V. M. Weaver, “Human breast cancer invasion and aggression correlates with ecm stiffening and immune cell infiltration,” *Integrative Biology*, vol. 7, no. 10, pp. 1120–1134, 2015. [Online]. Available: <http://dx.doi.org/10.1039/C5IB00040H>
- [3] A. J. Rice, E. Cortes, D. Lachowski, B. C. H. Cheung, S. A. Karim, J. P. Morton, and R. A. del Hernandez, “Matrix stiffness induces epithelialmesenchymal transition and promotes chemoresistance in pancreatic cancer cells,” *Oncogenesis*, vol. 6, no. 7, 2017. [Online]. Available: <http://dx.doi.org/10.1038/oncis.2017.54>
- [4] M. Guvendiren and J. A. Burdick, “Stiffening hydrogels to probe short- and long-term cellular responses to dynamic mechanics,” *Nature Communications*, vol. 3, no. 1, p. 792, 2012. [Online]. Available: <http://dx.doi.org/10.1038/ncomms1792>
- [5] A. M. Handorf, Y. Zhou, M. A. Halanski, and W. J. Li, “Tissue stiffness dictates development, homeostasis, and disease progression,” *Organogenesis*, vol. 11, no. 1, pp. 1–15, 2015. [Online]. Available: <https://www.ncbi.nlm.nih.gov/pubmed/25915734>
- [6] M. C. Lampi and C. A. Reinhart-King, “Targeting extracellular matrix stiffness to attenuate disease: From molecular mechanisms to clinical trials,” *Science Translational Medicine*, vol. 10, no. 422, 2018. [Online]. Available: <http://dx.doi.org/10.1126/scitranslmed.aao0475>
- [7] L. Wullkopf, A. V. West, N. Leijnse, T. R. Cox, C. D. Madsen, L. B. Oddershede, and J. T. Erler, “Cancer cells’ ability to mechanically adjust to extracellular matrix stiffness correlates with their invasive potential,” *Mol Biol Cell*, vol. 29, no. 20, pp. 2378–2385, 2018. [Online]. Available: <https://www.ncbi.nlm.nih.gov/pubmed/30091653>
- [8] A. J. Steward and D. J. Kelly, “Mechanical regulation of mesenchymal stem cell differentiation,” *Journal of Anatomy*, vol. 227, no. 6, pp. 717–731, 2015. [Online]. Available: <http://dx.doi.org/10.1111/joa.12243>

- [9] L.-S. Wang, J. E. Chung, P. P.-Y. Chan, and M. Kurisawa, "Injectable biodegradable hydrogels with tunable mechanical properties for the stimulation of neurogenic differentiation of human mesenchymal stem cells in 3d culture," *Biomaterials*, vol. 31, no. 6, 2010. [Online]. Available: <http://dx.doi.org/10.1016/j.biomaterials.2009.10.042>
- [10] P. M. Gilbert, K. L. Havenstrite, K. E. G. Magnusson, A. Sacco, N. A. Leonardi, P. Kraft, N. K. Nguyen, S. Thrun, M. P. Lutolf, and H. M. Blau, "Substrate elasticity regulates skeletal muscle stem cell self-renewal in culture," *Science*, vol. 329, no. 5995, pp. 1078–1081, 2010. [Online]. Available: <http://dx.doi.org/10.1126/science.1191035>
- [11] O. Chaudhuri, L. Gu, D. Klumpers, M. Darnell, S. A. Bencherif, J. C. Weaver, N. Huebsch, H.-p. Lee, E. Lippens, G. N. Duda, and D. J. Mooney, "Hydrogels with tunable stress relaxation regulate stem cell fate and activity," *Nature Materials*, vol. 15, no. 3, pp. 326–334, 2015. [Online]. Available: <http://dx.doi.org/10.1038/nmat4489>
- [12] O. Chaudhuri, L. Gu, M. Darnell, D. Klumpers, S. A. Bencherif, J. C. Weaver, N. Huebsch, and D. J. Mooney, "Substrate stress relaxation regulates cell spreading," *Nature Communications*, vol. 6, no. 1, p. 6365, 2015. [Online]. Available: <http://dx.doi.org/10.1038/ncomms7365>
- [13] O. Chaudhuri, "Viscoelastic hydrogels for 3d cell culture," *Biomaterials Science*, vol. 5, no. 8, pp. 1480–1490, 2017. [Online]. Available: <http://dx.doi.org/10.1039/C7BM00261K>
- [14] A. Bauer, L. Gu, B. Kwee, W. Li, M. Dellacherie, A. D. Celiz, and D. J. Mooney, "Hydrogel substrate stress-relaxation regulates the spreading and proliferation of mouse myoblasts," *Acta Biomaterialia*, vol. 62, 2017. [Online]. Available: <http://dx.doi.org/10.1016/j.actbio.2017.08.041>
- [15] K. M. Wisdom, K. Adebowale, J. Chang, J. Y. Lee, S. Nam, R. Desai, N. S. Rossen, M. Rafat, R. B. West, L. Hodgson, and O. Chaudhuri, "Matrix mechanical plasticity regulates cancer cell migration through confining microenvironments," *Nat Commun*, vol. 9, no. 1, p. 4144, 2018. [Online]. Available: <https://www.ncbi.nlm.nih.gov/pubmed/30297715>
- [16] H. Liu, H. D. Nguyen, and C. Lin, "Dynamic pegpeptide hydrogels via visible light and fmninduced tyrosine dimerization," *Advanced Healthcare Materials*, vol. 7, no. 22, p. 1800954, 2018. [Online]. Available: <http://dx.doi.org/10.1002/adhm.201800954>
- [17] X. Bi, A. Liang, Y. Tan, P. Maturavongsadit, A. Higginbotham, T. Gado, A. Gramling, H. Bahn, and Q. Wang, "Thiol-ene crosslinking polyamidoamine dendrimer-hyaluronic acid hydrogel system for biomedical applications," *J Biomater Sci Polym Ed*, vol. 27, no. 8, pp. 743–57, 2016. [Online]. Available: <https://www.ncbi.nlm.nih.gov/pubmed/26923639>
- [18] P. Lundberg, A. Bruin, J. W. Klijnstra, A. M. Nystrom, M. Johansson, M. Malkoch, and A. Hult, "Poly(ethylene glycol)-based thiol-ene hydrogel coatings-curing chemistry, aqueous stability, and potential marine antifouling applications," *ACS Appl Mater Interfaces*, vol. 2, no. 3, pp. 903–12, 2010. [Online]. Available: <https://www.ncbi.nlm.nih.gov/pubmed/20356297>

- [19] M. Patenaude, S. Campbell, D. Kinio, and T. Hoare, "Tuning gelation time and morphology of injectable hydrogels using ketone-hydrazide cross-linking," *Biomacromolecules*, vol. 15, no. 3, pp. 781–90, 2014. [Online]. Available: <https://www.ncbi.nlm.nih.gov/pubmed/24432725>
- [20] H. Qian and I. Aprahamian, "An emissive and ph switchable hydrazone-based hydrogel," *Chem Commun (Camb)*, vol. 51, no. 56, pp. 11158–61, 2015. [Online]. Available: <https://www.ncbi.nlm.nih.gov/pubmed/25989245>
- [21] S. L. Banerjee and N. K. Singha, "A new class of dual responsive self-healable hydrogels based on a core crosslinked ionic block copolymer micelle prepared via raft polymerization and diels-alder "click" chemistry," *Soft Matter*, vol. 13, no. 47, pp. 9024–9035, 2017. [Online]. Available: <https://www.ncbi.nlm.nih.gov/pubmed/29177283>
- [22] S. Tang, H. Ma, H. Tu, H. Wang, P. Lin, and K. S. Anseth, "Adaptable fast relaxing boronatebased hydrogels for probing cellmatrix interactions," *Advanced Science*, vol. 5, no. 9, p. 1800638, 2018. [Online]. Available: <http://dx.doi.org/10.1002/advs.201800638>
- [23] B. D. Fairbanks, M. P. Schwartz, A. E. Halevi, C. R. Nuttelman, C. N. Bowman, and K. S. Anseth, "A versatile synthetic extracellular matrix mimic via thiolnorbornene photopolymerization," *Advanced Materials*, vol. 21, no. 48, pp. 5005–5010, 2009. [Online]. Available: <http://dx.doi.org/10.1002/adma.200901808>
- [24] S. Singh, F. Topuz, K. Hahn, K. Albrecht, and J. Groll, "Embedding of active proteins and living cells in redoxsensitive hydrogels and nanogels through enzymatic crosslinking," *Angewandte Chemie International Edition*, vol. 52, no. 10, pp. 3000–3003, 2013. [Online]. Available: <http://dx.doi.org/10.1002/anie.201206266>
- [25] H. Shih and C. C. Lin, "Visible-light-mediated thiol-ene hydrogelation using eosin-y as the only photoinitiator," *Macromolecular Rapid Communications*, vol. 34, no. 3, pp. 269–273, 2013.
- [26] S. R. Zavada, N. R. McHardy, and T. F. Scott, "Oxygen-mediated enzymatic polymerization of thiolene hydrogels," *Journal of Materials Chemistry B*, vol. 2, no. 17, pp. 2598–2605, 2014. [Online]. Available: <http://dx.doi.org/10.1039/C3TB21794A>
- [27] A. Sundarakrishnan, E. Acero, J. Coburn, K. Chwalek, B. Partlow, and D. L. Kaplan, "Phenol red-silk tyrosine cross-linked hydrogels," *Acta Biomaterialia*, vol. 42, pp. 102–113, 2016. [Online]. Available: <http://dx.doi.org/10.1016/j.actbio.2016.06.020>
- [28] B. P. Partlow, C. W. Hanna, J. RnjakKovacina, J. E. Moreau, M. B. Applegate, K. A. Burke, B. Marelli, A. N. Mitropoulos, F. G. Omenetto, and D. L. Kaplan, "Highly tunable elastomeric silk biomaterials," *Advanced Functional Materials*, vol. 24, no. 29, pp. 4615–4624, 2014.
- [29] K. Xu, K. Narayanan, F. Lee, K. Bae, S. Gao, and M. Kurisawa, "Enzyme-mediated hyaluronic acidtyramine hydrogels for the propagation of human embryonic stem cells in 3d," *Acta Biomaterialia*, vol. 24, pp. 159–171, 2015.

- [30] Y. Lee, K.-H. Choi, K. Park, J.-M. Lee, B. Park, and K. Park, "In situ forming and h₂O₂-releasing hydrogels for treatment of drug-resistant bacterial infections," *ACS Applied Materials & Interfaces*, 2017. [Online]. Available: <http://dx.doi.org/10.1021/acsami.7b03870>
- [31] S. Sakai, M. Tsumura, M. Inoue, Y. Koga, K. Fukano, and M. Taya, "Polyvinyl alcohol-based hydrogel dressing gellable on-wound via a co-enzymatic reaction triggered by glucose in the wound exudate," *Journal of Materials Chemistry B*, vol. 1, no. 38, pp. 5067–5075, 2013. [Online]. Available: <http://dx.doi.org/10.1039/C3TB20780C>
- [32] K. Ren, B. Li, Q. Xu, C. Xiao, C. He, G. Li, and X. Chen, "Enzymatically crosslinked hydrogels based on linear poly(ethylene glycol) polymer: performance and mechanism," *Polymer Chemistry*, vol. 8, no. 45, pp. 7017–7024, 2017. [Online]. Available: <http://dx.doi.org/10.1039/C7PY01597F>
- [33] D. Wang, X. Yang, Q. Liu, L. Yu, and J. Ding, "Enzymatically cross-linked hydrogels based on a linear poly(ethylene glycol) analogue for controlled protein release and 3d cell culture," *Journal of Materials Chemistry B*, 2018. [Online]. Available: <http://dx.doi.org/10.1039/C8TB01949E>
- [34] E. Oh, J. E. Oh, J. Hong, Y. Chung, Y. Lee, K. D. Park, S. Kim, and C. O. Yun, "Optimized biodegradable polymeric reservoir-mediated local and sustained co-delivery of dendritic cells and oncolytic adenovirus co-expressing il-12 and gm-csf for cancer immunotherapy," *J Control Release*, vol. 259, pp. 115–127, 2017. [Online]. Available: <https://www.ncbi.nlm.nih.gov/pubmed/28336378>
- [35] T. Thi, Y. Lee, S. Ryu, H.-J. Sung, and K. Park, "Oxidized cyclodextrin-functionalized injectable gelatin hydrogels as a new platform for tissue-adhesive hydrophobic drug delivery," *RSC Advances*, vol. 7, no. 54, pp. 34 053–34 062, 2017. [Online]. Available: <http://dx.doi.org/10.1039/C7RA04137C>
- [36] B. Kim, Y. Lee, J. Son, K. Park, and K. Park, "Dual enzymetriggered in situ crosslinkable gelatin hydrogels for artificial cellular microenvironments," *Macromolecular Bioscience*, vol. 16, no. 11, pp. 1570–1576, 2016. [Online]. Available: <http://dx.doi.org/10.1002/mabi.201600312>
- [37] S. Sakai, K. Ueda, E. Gantumur, M. Taya, and M. Nakamura, "Drop on drop multimaterial 3d bioprinting realized by peroxidasemediated crosslinking," *Macromolecular Rapid Communications*, vol. 39, no. 3, p. 1700534, 2018. [Online]. Available: <http://dx.doi.org/10.1002/marc.201700534>
- [38] E. Gantumur, S. Sakai, M. Nakahata, and M. Taya, "Cytocompatible enzymatic hydrogelation mediated by glucose and cysteine residues," *ACS Macro Letters*, pp. 485–488, 2017. [Online]. Available: <http://dx.doi.org/10.1021/acsmacrolett.7b00122>
- [39] S. E. Vidal, K. A. Tamamoto, H. Nguyen, R. D. Abbott, D. M. Cairns, and D. L. Kaplan, "3d biomaterial matrix to support long term, full thickness, immuno-competent human skin equivalents with nervous system components," *Biomaterials*, 2018. [Online]. Available: <http://dx.doi.org/10.1016/j.biomaterials.2018.04.044>

- [40] Y. Lee, D. A. Balikov, J. Lee, S. Lee, S. Lee, J. Lee, K. Park, and H.-J. Sung, "In situ forming gelatin hydrogels-directed angiogenic differentiation and activity of patient-derived human mesenchymal stem cells," *International Journal of Molecular Sciences*, vol. 18, no. 8, p. 1705, 2017. [Online]. Available: <http://dx.doi.org/10.3390/ijms18081705>
- [41] S. Kobayashi, H. Uyama, and S. Kimura, "Enzymatic polymerization," *Chemical Reviews*, vol. 101, no. 12, pp. 3793–3818, 2001. [Online]. Available: <http://dx.doi.org/10.1021/cr9901211>
- [42] Z. Liu, Y. Lv, A. Zhu, and Z. An, "One-enzyme triple catalysis: Employing the promiscuity of horseradish peroxidase for synthesis and functionalization of well-defined polymers," *ACS Macro Letters*, vol. 7, no. 1, pp. 1–6, 2017.
- [43] J. Carthew, J. E. Frith, and F.-J. S. of Materials, "Polyethylene glycolgelatin hydrogels with tuneable stiffness prepared by horseradish peroxidase-activated tetrazinenorborene ligation," *Journal of Materials*, 2018. [Online]. Available: <http://dx.doi.org/10.1039/C7TB02764H>
- [44] K. R. Levental, H. Yu, L. Kass, J. N. Lakins, M. Egeblad, J. T. Erler, S. F. Fong, K. Csiszar, A. Giaccia, W. Weninger, M. Yamauchi, D. L. Gasser, and V. M. Weaver, "Matrix crosslinking forces tumor progression by enhancing integrin signaling," *Cell*, vol. 139, no. 5, pp. 891–906, 2009. [Online]. Available: <https://www.ncbi.nlm.nih.gov/pubmed/19931152>
- [45] Y. C. Choi, J. S. Choi, Y. J. Jung, and Y. W. Cho, "Human gelatin tissue-adhesive hydrogels prepared by enzyme-mediated biosynthesis of dopa and fe³⁺ ion crosslinking," *J. Mater. Chem. B*, vol. 2, 2014.
- [46] G. Springsteen and B. Wang, "A detailed examination of boronic aciddiol complexation," *Tetrahedron*, vol. 58, no. 26, pp. 5291–5300, 2002. [Online]. Available: [http://dx.doi.org/10.1016/S0040-4020\(02\)00489-1](http://dx.doi.org/10.1016/S0040-4020(02)00489-1)
- [47] M. E. Smithmyer, C. C. Deng, S. E. Cassel, P. J. LeValley, B. S. Sumerlin, and A. M. Kloxin, "Self-healing boronic acid-based hydrogels for 3d co-cultures," *ACS Macro Letters*, pp. 1105–1110, 2018. [Online]. Available: <http://dx.doi.org/10.1021/acsmacrolett.8b00462>
- [48] C. C. Deng, W. Brooks, K. A. Abboud, and B. S. Sumerlin, "Boronic acid-based hydrogels undergo self-healing at neutral and acidic ph," *ACS Macro Letters*, vol. 4, no. 2, pp. 220–224, 2015. [Online]. Available: <http://dx.doi.org/10.1021/acsmacrolett.5b00018>
- [49] F. Zhao, D. Wu, D. Yao, R. Guo, W. Wang, A. Dong, D. Kong, and J. Zhang, "An injectable particle-hydrogel hybrid system for glucose-regulatory insulin delivery," *Acta Biomaterialia*, vol. 64, pp. 334–345, 2017. [Online]. Available: <http://dx.doi.org/10.1016/j.actbio.2017.09.044>
- [50] V. Yesilyurt, M. J. Webber, E. A. Appel, C. Godwin, R. Langer, and D. G. Anderson, "Injectable selfhealing glucoseresponsive hydrogels with phregulated mechanical properties," *Advanced Materials*, vol. 28, no. 1, pp. 86–91, 2015. [Online]. Available: <http://dx.doi.org/10.1002/adma.201502902>

- [51] J. V. Accardo and J. A. Kalow, "Reversibly tuning hydrogel stiffness through photocontrolled dynamic covalent crosslinks," *Chemical Science*, vol. 9, no. 27, pp. 5987–5993, 2018. [Online]. Available: <http://dx.doi.org/10.1039/C8SC02093K>
- [52] V. Yesilyurt, A. M. Ayoob, E. A. Appel, J. T. Borenstein, R. Langer, and D. G. Anderson, "Mixed reversible covalent crosslink kinetics enable precise, hierarchical mechanical tuning of hydrogel networks," *Advanced Materials*, vol. 29, no. 19, p. 1605947, 2017. [Online]. Available: <http://dx.doi.org/10.1002/adma.201605947>
- [53] E. Montanari, M. Pelliccia, A. Gennari, L. Manzi, R. Donno, N. J. Oldham, A. MacDonald, and N. Tirelli, "Tyrosinase-assisted bioconjugation. a versatile approach to chimeric macromolecules," *Bioconjugate Chemistry*, 2018. [Online]. Available: <http://dx.doi.org/10.1021/acs.bioconjchem.8b00227>
- [54] B. D. Fairbanks, M. P. Schwartz, C. N. Bowman, and K. S. Anseth, "Photoinitiated polymerization of peg-diacrylate with lithium phenyl-2,4,6-trimethylbenzoylphosphinate: polymerization rate and cytocompatibility," *Biomaterials*, vol. 30, no. 35, pp. 6702–7, 2009. [Online]. Available: <https://www.ncbi.nlm.nih.gov/pubmed/19783300>
- [55] Z. Mnoz, H. Shih, and L.-C. C. Science, "Gelatin hydrogels formed by orthogonal thiol-norbornene photochemistry for cell encapsulation," *Biomaterials Science*, 2014. [Online]. Available: <http://dx.doi.org/10.1039/C4BM00070F>
- [56] A. J. Steward and D. J. Kelly, "Mechanical regulation of mesenchymal stem cell differentiation," *J Anat*, vol. 227, no. 6, pp. 717–31, 2015. [Online]. Available: <https://www.ncbi.nlm.nih.gov/pubmed/25382217>
- [57] N. Huebsch, P. R. Arany, A. S. Mao, D. Shvartsman, O. A. Ali, S. A. Bencherif, J. Rivera-Feliciano, and D. J. Mooney, "Harnessing traction-mediated manipulation of the cell/matrix interface to control stem-cell fate," *Nat Mater*, vol. 9, no. 6, pp. 518–26, 2010. [Online]. Available: <https://www.ncbi.nlm.nih.gov/pubmed/20418863>
- [58] A. J. Engler, S. Sen, H. L. Sweeney, and D. E. Discher, "Matrix elasticity directs stem cell lineage specification," *Cell*, vol. 126, no. 4, pp. 677–89, 2006. [Online]. Available: <https://www.ncbi.nlm.nih.gov/pubmed/16923388>
- [59] K. Moriyama, K. Minamihata, R. Wakabayashi, M. Goto, and N. Kamiya, "Enzymatic preparation of a redox-responsive hydrogel for encapsulating and releasing living cells," *Chemical Communications*, vol. 50, no. 44, pp. 5895–5898, 2014. [Online]. Available: <http://dx.doi.org/10.1039/C3CC49766F>
- [60] H. Shih, H. Y. Liu, and C. C. Lin, "Improving gelation efficiency and cytocompatibility of visible light polymerized thiol-norbornene hydrogels via addition of soluble tyrosine," *Biomater Sci*, vol. 5, no. 3, pp. 589–599, 2017. [Online]. Available: <https://www.ncbi.nlm.nih.gov/pubmed/28174779>
- [61] M. Mishina, K. Minamihata, K. Moriyama, and T. Nagamune, "Peptide tag-induced horseradish peroxidase-mediated preparation of a streptavidin-immobilized redox-sensitive hydrogel," *Biomacromolecules*, vol. 17, no. 6, pp. 1978–84, 2016. [Online]. Available: <https://www.ncbi.nlm.nih.gov/pubmed/27183298>

- [62] H. Zhang, Y. Xu, J. Joseph, and B. Kalyanaraman, "Intramolecular electron transfer between tyrosyl radical and cysteine residue inhibits tyrosine nitration and induces thiyl radical formation in model peptides treated with myeloperoxidase, h₂o₂, and no₂- epr spin trapping studies," *Journal of Biological Chemistry*, vol. 280, no. 49, pp. 40 684–40 698, 2005. [Online]. Available: <http://dx.doi.org/10.1074/jbc.M504503200>
- [63] B. E. Sturgeon, H. J. Sipe, D. P. Barr, J. T. Corbett, J. G. Martinez, and R. P. Mason, "The fate of the oxidizing tyrosyl radical in the presence of glutathione and ascorbate implications for the radical sink hypothesis," *Journal of Biological Chemistry*, vol. 273, no. 46, pp. 30 116–30 121, 1998. [Online]. Available: <http://dx.doi.org/10.1074/jbc.273.46.30116>
- [64] N. Mogharrab, H. Ghourchian, and M. Amininasab, "Structural stabilization and functional improvement of horseradish peroxidase upon modification of accessible lysines: Experiments and simulation," *Biophysical Journal*, vol. 92, no. 4, pp. 1192–1203, 2007. [Online]. Available: <http://dx.doi.org/10.1529/biophysj.106.092858>
- [65] A. Henriksen, D. J. Schuller, K. Meno, and W.-K. G. Biochemistry, "Structural interactions between horseradish peroxidase c and the substrate benzhydroxamic acid determined by x-ray crystallography," *Biochemistry*, 1998. [Online]. Available: <http://dx.doi.org/10.1021/bi980234j>
- [66] K. J. Baynton, J. K. Bewtra, N. Biswas, and K. E. Taylor, "Inactivation of horseradish peroxidase by phenol and hydrogen peroxide: a kinetic investigation," *Biochim Biophys Acta*, vol. 1206, no. 2, pp. 272–8, 1994. [Online]. Available: <https://www.ncbi.nlm.nih.gov/pubmed/8003531>
- [67] J. Hernandez-Ruiz, M. B. Arnao, A. N. Hiner, F. Garcia-Canovas, and M. Acosta, "Catalase-like activity of horseradish peroxidase: relationship to enzyme inactivation by h₂o₂," *Biochem J*, vol. 354, no. Pt 1, pp. 107–14, 2001. [Online]. Available: <https://www.ncbi.nlm.nih.gov/pubmed/11171085>
- [68] S. Sakai, K. Komatani, and M. Taya, "Glucose-triggered co-enzymatic hydrogelation of aqueous polymer solutions," *RSC Adv.*, vol. 2, no. 4, pp. 1502–1507, 2012.
- [69] M. Khanmohammadi, M. B. Dastjerdi, A. Ai, A. Ahmadi, A. Godarzi, A. Rahimi, and J. Ai, "Horseradish peroxidase-catalyzed hydrogelation for biomedical applications," *Biomater Sci*, vol. 6, no. 6, pp. 1286–1298, 2018. [Online]. Available: <https://www.ncbi.nlm.nih.gov/pubmed/29714366>
- [70] R. Jin, C. Lin, and A. Cao, "Enzyme-mediated fast injectable hydrogels based on chitosanglycolic acid/tyrosine: preparation, characterization, and chondrocyte culture," *Polym. Chem.*, vol. 5, no. 2, pp. 391–398, 2014.
- [71] S. H. Kim, S. H. Lee, J. E. Lee, S. J. Park, K. Kim, I. S. Kim, Y. S. Lee, N. S. Hwang, and B. G. Kim, "Tissue adhesive, rapid forming, and sprayable ecm hydrogel via recombinant tyrosinase crosslinking," *Biomaterials*, vol. 178, pp. 401–412, 2018. [Online]. Available: <https://www.ncbi.nlm.nih.gov/pubmed/29752077>

- [72] R. Jin, B. Lou, and C. Lin, “Tyrosinase-mediated in situ forming hydrogels from biodegradable chondroitin sulfate-tyramine conjugates,” *Polymer International*, vol. 62, no. 3, pp. 353–361, 2013.
- [73] A. Coskun and E. U. Akkaya, “Three-point recognition and selective fluorescence sensing of l-dopa,” *Org Lett*, vol. 6, no. 18, pp. 3107–9, 2004. [Online]. Available: <https://www.ncbi.nlm.nih.gov/pubmed/15330599>
- [74] Y. Lee, J. Son, J. Kang, K. Park, and K. Park, “Hydrogen peroxide-releasing hydrogels for enhanced endothelial cell activities and neovascularization,” *ACS Applied Materials & Interfaces*, 2018. [Online]. Available: <http://dx.doi.org/10.1021/acsami.8b04522>

APPENDIX

APPENDIX

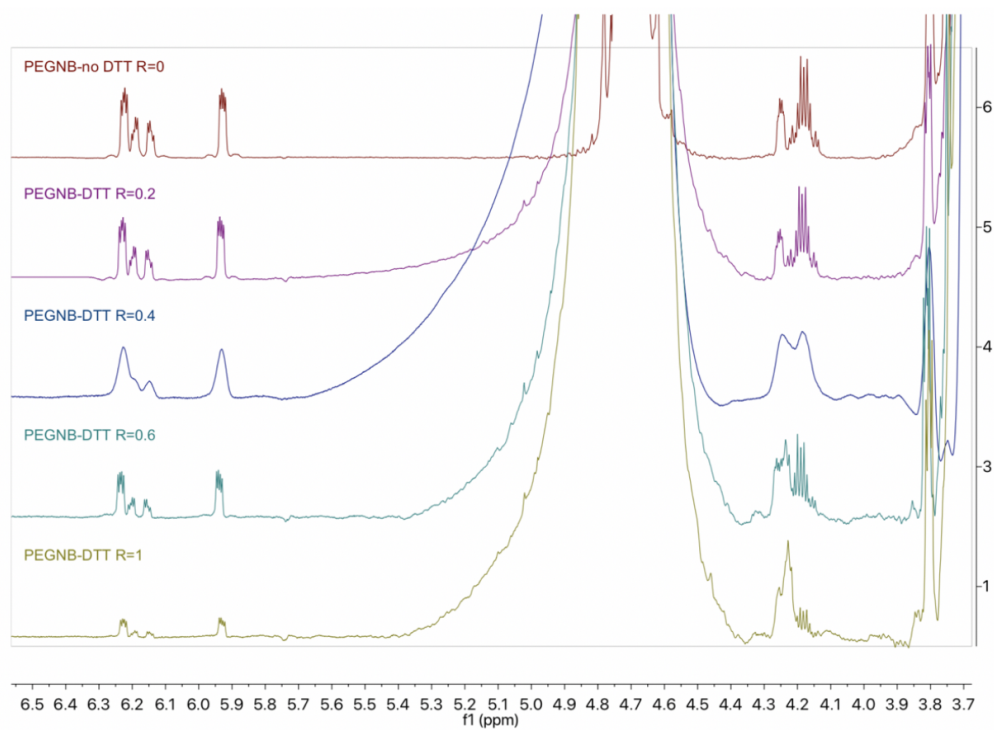


Fig. A.1: ^1H NMR spectra showing the consumption of the alkene proton (5.9-6.25 ppm) on the norbornene functional groups at different $R_{\text{thiol/norbornene}}$.